

Adaptive Local Clustering over Attributed Graphs

Technical Report

Haoran Zheng
Hong Kong Baptist University
Hong Kong SAR, China
cshrzeng@comp.hkbu.edu.hk

Renchi Yang
Hong Kong Baptist University
Hong Kong SAR, China
renchi@hkbu.edu.hk

Jianliang Xu
Hong Kong Baptist University
Hong Kong SAR, China
xujl@hkbu.edu.hk

Abstract—Given a graph \mathcal{G} and a seed node v_s , the objective of local graph clustering (LGC) is to identify a subgraph $C_s \in \mathcal{G}$ (a.k.a. local cluster) surrounding v_s in time roughly linear with the size of C_s . This approach yields personalized clusters without needing to access the entire graph, which makes it highly suitable for numerous applications involving large graphs. However, most existing solutions merely rely on the topological connectivity between nodes in \mathcal{G} , rendering them vulnerable to missing or noisy links that are commonly present in real-world graphs.

To address this issue, this paper resorts to leveraging the complementary nature of graph topology and node attributes to enhance local clustering quality. To effectively exploit the attribute information, we first formulate the LGC as an estimation of the *bidirectional diffusion distribution* (BDD), which is specialized for capturing the multi-hop affinity between nodes in the presence of attributes. Furthermore, we propose **LACA**, an efficient and effective approach for LGC that achieves superb empirical performance on multiple real datasets while maintaining strong locality. The core components of **LACA** include (i) a fast and theoretically-grounded preprocessing technique for node attributes, (ii) an adaptive algorithm for diffusing any vectors over \mathcal{G} with rigorous theoretical guarantees and expedited convergence, and (iii) an effective three-step scheme for BDD approximation. Extensive experiments, comparing 17 competitors on 8 real datasets, show that **LACA** outperforms all competitors in terms of result quality measured against ground truth local clusters, while also being up to orders of magnitude faster.

Index Terms—local cluster, attributes, graph diffusion, adaptive algorithm

I. INTRODUCTION

Local graph clustering (LGC) seeks to identify a single cluster (a.k.a. *local cluster*) pertinent to a given seed node by exploring a small region around it in the input graph. Compared to its global counterparts, LGC runs in time proportional to the size of its resulting cluster, regardless of the overall size of the input graph, making it particularly suitable for analyzing large-scale graphs, such as social networks, online shopping graphs, biological networks, and more. In practice, LGC finds extensive applications in various domains, including community detection or recommendation on social media [1]–[3], protein grouping in bioinformatics [4], [5], product return or user action prediction [6]–[8] on e-commerce platforms, and many others [9]–[13].

Canonical solutions for LGC [14]–[17] are predominantly based on random walk-based graph diffusion models [18], where the main idea is to spread mass from the seed node to other nodes along the edges. This methodology offers high

scalability and rigorous theoretical guarantees for complexity and output cluster size, but it is extremely sensitive to *structural heterogeneities* (e.g., high-degree nodes) in real networks, as pinpointed in [19], [20]. To mitigate this issue, subsequent LGC works [20]–[22] formulate LGC as a combinatorial optimization problem and leverage max flow algorithms to derive the “optimal” local clusters. Although these approaches improve the theoretical results of previous works, they are mostly of theoretical interest only and struggle to cope with sizable graphs due to poor practical efficiency. Most importantly, the above algorithms primarily focus on optimizing connectivity-based clustering quality metrics [23]. Real graphs are often constructed from data riddled with noise and thus encompass substantial noisy or missing links, leading to high ground-truth *conductance* [23], e.g., 0.765 for *Flickr* and 0.649 for *Yelp*. Consequently, applying classic LGC techniques to such graphs leads to sub-optimal performance, e.g., often low precisions below 30% (see Table V). As a partial remedy, recent efforts [24]–[27] incorporate *higher-order connectivity patterns* (e.g., motifs) into the LGC frameworks for improved clustering. However, they still rely solely on graph topology and are therefore vulnerable to missing or noisy nodes/edges. Moreover, these methods suffer from severe efficiency issues as they require enumerating the motifs in graphs in the pre-processing or on the fly.

In real life, graphs are often endowed with rich nodal attributes, e.g., user profiles in social networks and paper abstracts in citation graphs. These are termed *attributed graphs*. Recent studies [28]–[30] have corroborated that node attributes provide information that can effectively complement the graph topology for better performance in various tasks. Inspired by this, a straightforward idea is to exploit the attribute information to enhance LGC performance whilst retaining the *locality*. Very recently, several attempts [31]–[33] have been made to extend classic LGC techniques to attributed graphs by simply re-weighting each edge by the attribute similarity of its endpoints. However, this strategy merely accounts for connected nodes and still fails to deal with missing and noisy connections.

To tackle the foregoing issues, we propose **LACA**, a novel solution that seamlessly integrates node attributes into graph structures for effective LGC computation, while offering strong theoretical guarantees on locality and high empirical

efficiency. Specifically, LACA formulates the LGC task as a seeded random walk diffusion over graphs based on the novel notion of *bidirectional diffusion distribution* (BDD), an attribute-aware affinity measure dedicated to node pairs in attributed graphs. The main idea is to model the affinity between any node pair (v_s, v_t) as the expected normalized (exponential) cosine similarity (hereafter SNAS) between the attributes of ending node pairs of random walks originating from v_s and v_t , which essentially evaluates their *meeting probability* from the perspectives of both of them through random walks and attribute-based transitions. Accordingly, given a seed node v_s , the goal of LGC is to find a local cluster containing nodes with the highest BDD values w.r.t. v_s .

The exact computation of BDD incurs a significant cost of up to $O(n^3)$ as there are $n \times n$ possible ending node pairs from random walks starting at the seed node and any of the n nodes. This is *non-local* and infeasible for large graphs. In response, we develop an adaptive framework for an approximate solution with a runtime linear to the output size and independent of the size of the graph. First, we obtain a fast and theoretically grounded decomposition of the SNAS matrix into low-dimensional feature vectors through randomized techniques [34], [35]. This step enables the decoupling of the BDD computation and transforms the problem into the diffusion of vectors over input graphs. On top of that, we devise a new algorithm AdaptiveDiffuse, which diffuses non-negative vectors on graphs using efficient matrix operations in an adaptive fashion. It not only alleviates the intensive memory access patterns in previous traversal/sampling-based diffusion approaches [15], [36], [37] but also overcomes their limitations of sensitivity to high-degree nodes and slow convergence, without compromising the theoretical assurance in approximation and asymptotic performance. Lastly, a carefully designed three-step scheme is employed to construct the approximate BDD. We further conduct non-trivial theoretical analyses to reveal the approximation and complexity bounds of LACA, as well as its connection to *graph neural networks* (GNNs) [38].

Our empirical studies, which evaluate LACA against 17 competitors on 8 real attributed graph datasets with ground-truth local clusters, demonstrate that LACA is consistently superior or comparable with the state-of-the-art baseline approaches in terms of result quality at a fraction of their cost. In particular, on the largest *Amazon2M* dataset with 61.9 million edges, LACA is able to recover the target local clusters with an average of 1.8% improvement in precision and $152\times$ speedup compared to the best competitor.

II. PROBLEM FORMULATION

A. Notations and Terminology

Let $\mathcal{G} = (\mathcal{V}, \mathcal{E})$ be a connected, undirected, and unweighted graph (a.k.a. network), where $\mathcal{V} = \{v_1, v_2, \dots, v_n\}$ is a set of n nodes and $\mathcal{E} \in \mathcal{V} \times \mathcal{V}$ is a set of m edges. For each edge $(v_i, v_j) \in \mathcal{E}$, we say v_i and v_j are neighbors to each other. We use $\mathcal{N}(v_i)$ to denote the set of neighbors of v_i and $d(v_i) = |\mathcal{N}(v_i)|$ as its degree. Let \mathbf{A} be the adjacency matrix of \mathcal{G} where $\mathbf{A}_{i,j} = 1$ if $(v_i, v_j) \in \mathcal{E}$, otherwise $\mathbf{A}_{i,j} = 0$. The

TABLE I: Frequently used notations.

Notation	Description
$\mathcal{V}, \mathcal{E}, \mathbf{X}$	The node set, edge set, and node attribute matrix \mathbf{X} of attributed graph \mathcal{G} , respectively.
n, m, d	The numbers of nodes, edges, and distinct attributes, respectively.
$\mathcal{N}(v_i), d(v_i)$	The set of neighbors and degree of node v_i , respectively.
$\mathbf{A}, \mathbf{D}, \mathbf{P}$	The adjacency, degree, and transition matrices of the graph \mathcal{G} , respectively.
$\text{vol}(\mathcal{C})$	The volume of a set \mathcal{C} of nodes, i.e., $\sum_{v_i \in \mathcal{C}} d(v_i)$.
$\text{supp}(\vec{\mathbf{x}})$	The support of vector $\vec{\mathbf{x}}$, i.e., $\{i : \vec{\mathbf{x}}_i \neq 0\}$.
α	The restart factor in RWR, $\alpha \in (0, 1)$.
$s(v_i, v_j)$	The SNAS defined by Eq. (1).
$\pi(v_x, v_y)$	The RWR score of v_y w.r.t. v_x (See Eq. (6)).
$\vec{\rho}_t, \vec{\rho}'_t$	The exact and approximate BDD values of v_t w.r.t. v_s respectively (See definition in Eq. (5)).
$\mathbf{Z}, \vec{\mathbf{z}}^{(i)}$	The TNAM and its i -th row vector (See Eq. (10)).
ϵ, σ	The diffusion threshold and balancing parameter in Algo. 2.
k	The dimension of TNAM vectors $\vec{\mathbf{z}}^{(i)} \forall v_i \in \mathcal{V}$.

diagonal matrix \mathbf{D} is used to symbolize the degree matrix of \mathcal{G} where $\mathbf{D}_{i,i} = d(v_i)$. The *transition matrix* of \mathcal{G} is defined by $\mathbf{D}^{-1}\mathbf{A}$, where $\mathbf{P}_{i,j} = \frac{1}{d(v_i)}$ if $(v_i, v_j) \in \mathcal{E}$, otherwise $\mathbf{P}_{i,j} = 0$. Accordingly, $\mathbf{P}_{i,j}^\ell$ signifies the probability of a length- ℓ random walk originating from node v_i ending at node v_j .

A graph is referred to as an *attributed graph* if each node v_i in \mathcal{V} is endowed with a d -dimensional attribute vector $\vec{\mathbf{x}}^{(i)}$, which is the i -th row vector in the node attribute matrix \mathbf{X} of \mathcal{G} . We assume $\vec{\mathbf{x}}^{(i)}$ is L_2 -normalized, i.e., $\|\vec{\mathbf{x}}^{(i)}\|_2 = 1$. $\mathbf{X}_{i,j}$ and $\vec{\mathbf{x}}_j^{(i)}$ represent the (i, j) -th element in matrix \mathbf{X} and j -th entry in vector $\vec{\mathbf{x}}^{(i)}$, respectively. The *support* of vector $\vec{\mathbf{x}}^{(i)}$ is defined as $\text{supp}(\vec{\mathbf{x}}^{(i)}) = \{j : \vec{\mathbf{x}}_j^{(i)} \neq 0\}$, which comprises the indices of non-zero entries in $\vec{\mathbf{x}}^{(i)}$. The *volume* of a set \mathcal{C} of nodes is defined as $\text{vol}(\mathcal{C}) = \sum_{v_i \in \mathcal{C}} d(v_i)$. Given a length- n vector $\vec{\mathbf{x}}$, its *volume* $\text{vol}(\vec{\mathbf{x}})$ is defined as $\sum_{i \in \text{supp}(\vec{\mathbf{x}})} d(v_i)$. Table I lists notations frequently used throughout this paper.

A *local cluster* \mathcal{C}_s w.r.t. a seed node v_s in graph \mathcal{G} is defined as a subset of \mathcal{V} containing v_s . Intuitively, in an attributed graph \mathcal{G} , a good local cluster should be internally cohesive and well-separated from the remainder of \mathcal{G} in terms of both topological connections and attribute similarity. Given the seed node v_s , the general goal of LGC over attributed graph \mathcal{G} is to identify such a local cluster \mathcal{C}_s with the runtime cost roughly linear to its volume $\text{vol}(\mathcal{C}_s)$.

B. Symmetric Normalized Attribute Similarity

We quantify the the similarity of two nodes v_i and v_j in \mathcal{G} in terms of attributes as follows:

$$s(v_i, v_j) = \frac{f(\vec{\mathbf{x}}^{(i)}, \vec{\mathbf{x}}^{(j)})}{\sqrt{\sum_{v_\ell \in \mathcal{V}} f(\vec{\mathbf{x}}^{(i)}, \vec{\mathbf{x}}^{(\ell)})} \sqrt{\sum_{\vec{\mathbf{x}}^{(\ell)} \in \mathcal{V}} f(\vec{\mathbf{x}}^{(j)}, \vec{\mathbf{x}}^{(\ell)})}}, \quad (1)$$

where $f(\cdot, \cdot)$ can be any metric function defined over two vectors. The denominator in Eq. (1) is to ensure the $s(v_i, v_j)$ values w.r.t. any node $v_i \in \mathcal{V}$ to be symmetric and normalized to a comparable range ($0 \leq s(v_i, v_j) \leq 1$), which facilitates the design of the BDD in subsequent section. Particularly, $s(v_i, v_j)$ is referred to as the SNAS of nodes v_i and v_j .

We adopt two classic metric functions for $f(\cdot, \cdot)$, i.e., *cosine similarity* and *exponent cosine similarity* [39]. When $f(\cdot, \cdot)$

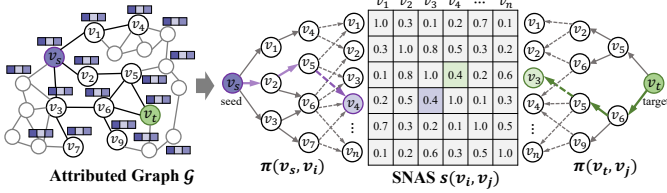


Fig. 1: Figurative Illustration of BDD.

is the cosine similarity, $f(\vec{x}^{(i)}, \vec{x}^{(j)}) = \vec{x}^{(i)} \cdot \vec{x}^{(j)}$ since $\|\vec{x}^{(i)}\|_2 = 1$. Then, the SNAS $s(v_i, v_j)$ can be computed via

$$\frac{\vec{x}^{(i)} \cdot \vec{x}^{(j)}}{\sqrt{\sum_{v_\ell \in \mathcal{V}} \vec{x}^{(i)} \cdot \vec{x}^{(\ell)}} \sqrt{\sum_{v_\ell \in \mathcal{V}} \vec{x}^{(j)} \cdot \vec{x}^{(\ell)}}}. \quad (2)$$

Analogously, when the exponent cosine similarity is adopted,

$$f(\vec{x}^{(i)}, \vec{x}^{(j)}) = \exp(\vec{x}^{(i)} \cdot \vec{x}^{(j)} / \delta) \quad (3)$$

and the SNAS of nodes v_i, v_j is formulated as

$$\frac{\exp(\vec{x}^{(i)} \cdot \vec{x}^{(j)} / \delta)}{\sqrt{\sum_{v_\ell \in \mathcal{V}} \exp(\vec{x}^{(i)} \cdot \vec{x}^{(\ell)} / \delta)} \sqrt{\sum_{v_\ell \in \mathcal{V}} \exp(\vec{x}^{(j)} \cdot \vec{x}^{(\ell)} / \delta)}, \quad (4)$$

where δ (typically 1 or 2) is the sensitivity factor. Essentially, Eq. (4) can be deemed as a variant of the *softmax function*.

C. Bidirectional Diffusion Distribution

We further propose the *bidirectional diffusion* (BDD) to model the likelihood of two nodes in \mathcal{G} to be in the same cluster. In particular, Unlike previous works that are based on biased graph proximity from the seed's view, BDD integrates the strength of topological connections and the attribute similarity of the node pair in a coherent framework from the perspectives of both the seed and target. More precisely, given a seed node $v_s \in \mathcal{V}$, for any target node $v_t \in \mathcal{V}$, the BDD $\vec{\rho}_t$ of node pair (v_s, v_t) is defined by

$$\vec{\rho}_t = \sum_{v_i, v_j \in \mathcal{V}} \pi(v_s, v_i) \cdot s(v_i, v_j) \cdot \pi(v_t, v_j), \quad (5)$$

where $s(v_i, v_j)$ is the SNAS of intermediate nodes v_i, v_j and

$$\pi(v_x, v_y) = \sum_{\ell=0}^{\infty} (1 - \alpha) \alpha^\ell \cdot \mathbf{P}_{x,y}^\ell \quad (6)$$

stands for the RWR (*random walk with restart* [40], [41]) score of node v_y w.r.t. node v_x . At each step, an RWR over \mathcal{G} either stops at the current node with $1 - \alpha$ probability or navigates to one of its neighbors uniformly at random with probability α . In essence, $\pi(v_s, v_i)$ (resp. $\pi(v_t, v_j)$) is the probability that an RWR originating from v_s (resp. v_t) terminates at node v_i (resp. v_j). Put differently, $\pi(v_s, v_i) \forall v_i \in \mathcal{V}$ (resp. $\pi(v_t, v_j) \forall v_j \in \mathcal{V}$) describe the distribution of mass (1.0 in total) disseminated from v_s (resp. v_t) to all the nodes in \mathcal{G} via random walks, respectively. Particularly, given a vector $\vec{a} \in \mathbb{R}^n$, we refer to the below process as an *RWR-based graph diffusion*:

$$\sum_{v_x \in \mathcal{V}} \vec{a}_x \cdot \pi(v_x, v_y) \quad \forall v_y \in \mathcal{V}, \quad (7)$$

where $\vec{a}_x \cdot \pi(v_x, v_y)$ can be interpreted as the amount of mass in \vec{a} spread from v_x to v_y via random walks on \mathcal{G} .

Let nodes (v_i, v_j) be the *ending node pair* of two bidirectional random walks with restart from seed node v_s and target node v_t . The BDD $\vec{\rho}_t$ of (v_s, v_t) in Eq. (5) is therefore

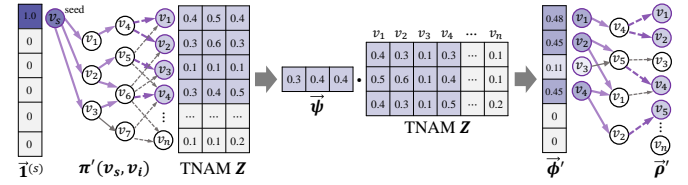


Fig. 2: Basic Idea of LACA.

the overall SNAS of all such ending pairs, as illustrated in Fig. 1. Intuitively, if two nodes v_s and v_t are located in the same cluster, their proximal nodes (i.e., nodes with high RWR scores) are more likely to have high SNAS (i.e., high attribute homogeneity), resulting in a high BDD value $\vec{\rho}_t$. Particularly, the injection of the SNAS reduces the likelihood of transiting to undesired nodes caused by noisy links, while increasing the affinity to desired nodes with high attribute similarities but low connectivity due to missing links.

Remark. When the input graph \mathcal{G} is *non-attributed*, we set the SNAS $s(v_i, v_j) = 1$ if $v_i = v_j$ and 0 otherwise $\forall v_i, v_j \in \mathcal{V}$. The BDD $\rho(v_q, v_t)$ is then a variant of the CoSimRank [42] metric, which measures the likelihood of random walks from two nodes meeting each other over the graph.

D. Problem Statement

Based thereon, the LGC task for seed node v_s over attributed graph \mathcal{G} is framed as an *approximation* of the BDD vector $\vec{\rho}$ (denoted as $\vec{\rho}'$), followed by a simple extraction of the nodes with $|\mathcal{C}_s|$ largest values in $\vec{\rho}'$ as the predicted local cluster \mathcal{C}_s . In turn, our major focus of the LGC problem lies in the computation of $\vec{\rho}'$. More formally, given a diffusion threshold ϵ , we aim to estimate a BDD vector $\vec{\rho}'$ such that both its output volume $\text{vol}(\vec{\rho}')$ (i.e., the size of the explored region on \mathcal{G}) and entailed computation cost are bounded by $O(1/\epsilon)$, i.e., achieving the locality.

Notice that the direct computation of BDD $\vec{\rho}$ in Eq. (5) requires the RWR scores $\pi(v_s, v_i)$ of all intermediate nodes $v_i \in \mathcal{V}$ w.r.t. the seed v_s , the RWR scores $\pi(v_t, v_j)$ of all intermediate nodes $v_j \in \mathcal{V}$ w.r.t. all possible target nodes $v_t \in \mathcal{V}$, and the SNAS values $s(v_i, v_j)$ of all possible node pairs $(v_i, v_j) \in \mathcal{V} \times \mathcal{V}$. The latter two ingredients involve up to $O(n^2)$ node pairs, rendering the *local* estimation of $\vec{\rho}$ particularly challenging. Additionally, it remains unclear how to provide approximation accuracy assurance for $\vec{\rho}'$.

III. SOLUTION OVERVIEW

To address the preceding technical challenges, we streamline the approximation of BDD via a three-step framework through our careful analyses as follows.

A. Problem Transformation

Firstly, by the definition of BDD in Eq. (5) and the symmetric property of RWR scores [43] (i.e., $\pi(v_i, v_j) \cdot d(v_i) = \pi(v_j, v_i) \cdot d(v_j)$), we can rewrite the BDD value $\vec{\rho}_t$ of any target node $v_t \in \mathcal{V}$ w.r.t. the seed node v_s as

$$\vec{\rho}_t = \frac{1}{d(v_t)} \sum_{v_i \in \mathcal{V}} \vec{\phi}_i \cdot \pi(v_i, v_t), \quad (8)$$

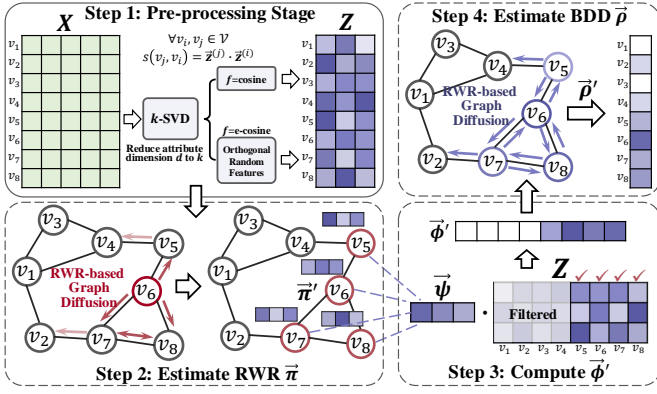


Fig. 3: Overview of LACA.

where $\vec{\phi}$ is called the RWR-SNAS vector w.r.t. v_s and

$$\vec{\phi}_i = \sum_{v_j \in \mathcal{V}} \pi(v_s, v_j) \cdot s(v_j, v_i) \cdot d(v_i). \quad (9)$$

Intuitively, if the RWR-SNAS vector $\vec{\phi}$ is at hand, Eq. (8) implies that an *approximate* BDD vector $\vec{\rho}'$ can be obtained via the RWR-based graph diffusion (see Eq. (7)) of $\vec{\phi}$ over the graph \mathcal{G} with a diffusion threshold.

However, the direct and exact computation of the RWR-SNAS vector $\vec{\phi}$ in Eq. (9) is still immensely expensive as it requires calculating the SNAS $s(v_j, v_i)$ for all possible node pairs (up to $O(n^2)$) in \mathcal{G} . Towards this end, we propose to decompose each SNAS $s(v_j, v_i)$ as the product of two length- k ($k \ll d$ and is a constant) vectors, i.e.,

$$s(v_j, v_i) = \vec{z}^{(j)} \cdot \vec{z}^{(i)}, \quad (10)$$

where $\mathbf{Z} \in \mathbb{R}^{n \times k}$ is a transformed node attribute matrix \vec{X} (hereafter TNAM). In doing so, the RWR-SNAS vector $\vec{\phi}$ in Eq. (9) can be reformulated as

$$\vec{\phi}_i = \vec{\pi} \cdot \mathbf{Z} \cdot \vec{z}^{(i)} \cdot d(v_i), \quad (11)$$

where $\vec{\pi}$ denotes the RWR vector w.r.t. seed node v_{s_s} , i.e., $\vec{\pi}_i = \pi(v_s, v_i) \forall v_i \in \mathcal{V}$. Given an estimation $\vec{\pi}'$ of $\vec{\pi}$, the term $\vec{\pi}' \cdot \mathbf{Z}$ in Eq. (11) can be approximated by

$$\vec{\psi} = \sum_{i \in \text{supp}(\vec{\pi}')} \vec{\pi}'_i \cdot \vec{z}^{(i)} \in \mathbb{R}^k, \quad (12)$$

and accordingly, we can estimate $\vec{\phi}$ by

$$\vec{\phi}_i = \vec{\psi} \cdot \vec{z}^{(i)} \cdot d(v_i) \quad \forall v_i \in \{v_i | i \in \text{supp}(\vec{\pi}')\}. \quad (13)$$

Note that $\vec{\psi}$ is shared by the computations of all possible $\vec{\phi}'_i$. If we can calculate an approximate RWR vector $\vec{\pi}'$ with support size (i.e., the number of non-zero entries) $\text{supp}(\vec{\pi}') = O(1/\epsilon)$ in $O(1/\epsilon)$ time, the construction times and support sizes of $\vec{\psi}$ and $\vec{\phi}'$ are also bounded by $O(1/\epsilon)$.

As illustrated in Fig. 2, our above idea transforms the computation of the BDD for each target node $v_t \in \mathcal{V}$ in Fig. 1 into (i) aggregation of TNAM vectors of nodes into vector $\vec{\psi}$ based on their RWR scores in $\vec{\pi}'$, (ii) construction of the RWR-SNAS vector $\vec{\phi}'$ by Eq. (13), and (iii) RWR-based graph diffusion of $\vec{\phi}'$ over \mathcal{G} to get $\vec{\rho}'$.

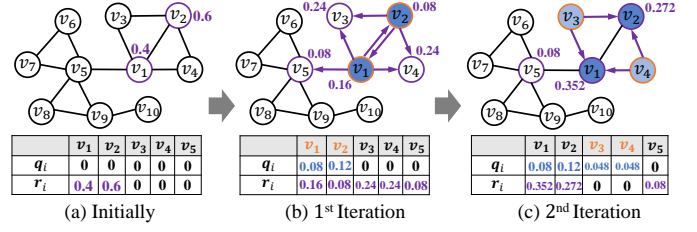


Fig. 4: GreedyDiffuse with $\alpha = 0.8$ and $\epsilon = 0.1$.

B. A Three-Step Framework

The BDD approximation thus involves four subtasks, i.e., the computations of the TNAM \mathbf{Z} , approximate RWR vector $\vec{\pi}'$, RWR-SNAS vector $\vec{\phi}'$, and approximate BDD vector $\vec{\rho}'$.

Since $\vec{\phi}'$ can be properly computed using Eq. (13), our main tasks are to construct \mathbf{Z} , $\vec{\pi}'$, and $\vec{\rho}'$. Let $\vec{1}^{(s)}$ be a vector with 1 at s -th entry and 0 everywhere else. The exact RWR score $\vec{\pi}'_t$ of any node $v_t \in \mathcal{V}$ can be represented as

$$\vec{\pi}'_t = \sum_{v_i \in \mathcal{V}} \vec{1}_i^{(s)} \cdot \pi(v_i, v_t),$$

which can also be regarded as an RWR-based graph diffusion. This inspires us to design a unified graph diffusion algorithm that obtains estimations $\vec{\pi}'$ and $\vec{\rho}'$ by diffusing $\vec{1}^{(s)}$ and $\vec{\phi}'$ over \mathcal{G} based on RWR, respectively, while fulfilling the volume and runtime bounds (i.e., $O(1/\epsilon)$), and high practical efficiency. As for TNAM \mathbf{Z} , we propose to generate it through a preprocessing of the input node attribute matrix \vec{X} as \mathbf{Z} can be reused in the LGC task of any seed node $v_s \in \mathcal{V}$.

As summarized in Fig. 3, our proposed LACA includes a preprocessing algorithm that converts \vec{X} into a k -dimensional TNAM \mathbf{Z} thereby enabling the problem transformation in Eq. (11) (Algo. 3), and a three-step scheme for the online approximation of BDD vector. Therein, Step 1 identifies a small set of nodes around the seed node by estimating their RWR $\vec{\pi}'$ using an RWR-based graph diffusion algorithm (Algo. 1 or 2) with $\vec{1}^{(s)}$ as input, while Step 2 aggregates their TNAM vectors as $\vec{\psi}$ (Eq. (12)) to build the RWR-SNAS vector $\vec{\phi}'$ (Eq. (11)). In the final step (Step 3), LACA conducts another RWR-based graph diffusion with $\vec{\phi}'$ over \mathcal{G} to derive the approximate BDD vector $\vec{\rho}'$ (Algo. 4).

In succeeding sections, we first elaborate on the algorithmic design of our generalized RWR-based graph diffusion approaches (Algo. 1 and 2) for the estimations of RWR vector $\vec{\pi}'$ and BDD vector $\vec{\rho}'$ in Section IV-C. After that, Section V describes the technical details of Algo. 3 for constructing TNAM \mathbf{Z} and the complete LACA algorithm (Algo. 4), followed by theoretical analyses in terms of accuracy approximation, volume, and runtime.

IV. RWR-BASED GRAPH DIFFUSION ALGORITHMS

We unify the computations of $\vec{\pi}'$ and $\vec{\rho}'$ as diffusing an input vector \vec{f} along edges over \mathcal{G} to get \vec{q} satisfying

$$\forall v_t \in \mathcal{V}, 0 \leq \sum_{v_i \in \mathcal{V}} \vec{f}_i \cdot \pi(v_i, v_t) - \vec{q}_t \leq \epsilon \cdot d(v_t), \quad (14)$$

Algorithm 1: GreedyDiffuse

Input: Transition matrix \mathbf{P} , restart factor α , diffusion threshold ϵ , initial vector \vec{f}

Output: Diffused vector \vec{q}

- 1 $\vec{r} \leftarrow \vec{f}; \vec{q} \leftarrow \mathbf{0};$
- 2 **while true do**
- 3 Compute sparse vector $\vec{\gamma};$ ▷ Eq. (15)
- 4 **if $\vec{\gamma}$ is $\mathbf{0}$ then break;**
- 5 $\vec{r} \leftarrow \vec{r} - \vec{\gamma};$
- 6 Update \vec{q} and $\vec{\gamma};$ ▷ Eq. (16)
- 7 $\vec{r} \leftarrow \vec{r} + \vec{\gamma};$
- 8 **return $\vec{q};$**

which is $\vec{\pi}'$ and $\vec{\rho}'$ when \vec{f} is set to $\vec{\mathbf{1}}^{(s)}$ and $\vec{\phi}'$, respectively. Instead of using deterministic graph traversals or random walk samples for diffusion as in prior algorithms [15], [36], we first develop GreedyDiffuse by leveraging matrix operations and a greedy strategy for cache-friendly memory access patterns and higher efficiency. Further, we upgrade GreedyDiffuse to AdaptiveDiffuse for faster termination without compromising the theoretical guarantees through an adaptive scheme.

A. The GreedyDiffuse Approach

Algo. 1 presents the pseudo-code of GreedyDiffuse for “diffusing” any initial non-negative vector \vec{f} . Algo. 1 is greedy in the sense that the diffusion operations are solely conducted for nodes whose residues are beyond a certain threshold so as to minimize the total amount of operations needed to satisfy the desired accuracy guarantee.

Given the transition matrix \mathbf{P} of the input graph \mathcal{G} and the diffusion threshold, Algo. 1 begins by initializing a *residual* vector \vec{r} as \vec{f} and a *reserve* vector \vec{q} as $\mathbf{0}$ at Line 1. Afterward, it starts an iterative process for diffusing and converting the residuals in \vec{r} , which continuously transfers the residuals into the reserve vector \vec{q} (Lines 2-7). Specifically, in each iteration, we first identify the residuals in \vec{r} whose corresponding $\vec{r}_i/d(v_i)$ values are equal to or beyond $\epsilon \cdot \|\vec{f}\|_1$ and move them to a temporary vector $\vec{\gamma}$ for subsequent diffusion. More precisely, we obtain a sparse vector $\vec{\gamma}$ at Line 3 as follows:

$$\vec{\gamma}_i = \begin{cases} \vec{r}_i & \text{if } (\vec{r} \mathbf{D}^{-1})_i = \frac{\vec{r}_i}{d(v_i)} \geq \epsilon, \\ 0 & \text{otherwise.} \end{cases} \quad (15)$$

Next, we update residual vector \vec{r} as $\vec{r} - \vec{\gamma}$ such that \vec{r} contain the residuals below the threshold and then convert $(1-\alpha)$ portion of residuals in $\vec{\gamma}$ into reserve vector \vec{q} (Lines 5-6). $\forall v_i \in \mathcal{V}$, its remaining α fraction of residual in $\vec{\gamma}$ is later evenly scattered to its out-neighbors. That is, each node $v_j \in \mathcal{V}$ receives a total of $\sum_{v_i \in \mathcal{N}(v_j)} \alpha \cdot \frac{\vec{\gamma}_i}{d(v_i)}$ residual from its incoming neighbors $\mathcal{N}(v_j)$, which can be written as a sparse matrix-vector multiplication as follows (Line 6):

$$\vec{q} \leftarrow \vec{q} + (1-\alpha)\vec{\gamma}, \quad \vec{r} \leftarrow \alpha\vec{\gamma}\mathbf{P} \quad (16)$$

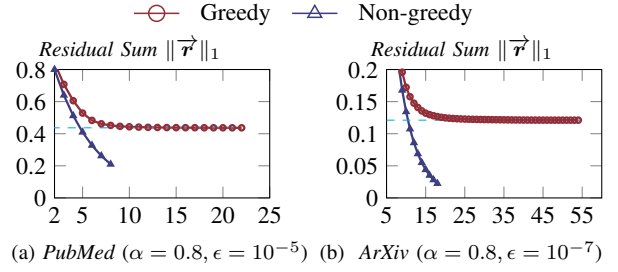


Fig. 5: Greedy v.s. Non-greedy.

These residuals in $\vec{\gamma}$ will be added back to \vec{r} for the next round of conversion and diffusion (Line 7).

Theorem IV.1. Given initial vector \vec{f} , restart factor α , and diffusion threshold ϵ , Algo. 1 outputs a diffused vector \vec{q} satisfying Eq. (14) using $O\left(\max\left\{|\text{supp}(\vec{f})|, \frac{\|\vec{f}\|_1}{(1-\alpha)\epsilon}\right\}\right)$ time.

Proof. All missing proofs can be found in Appendix A. \square

Algo. 1 repeats the above procedure until the resulting $\vec{\gamma}$ turns to be a zero vector (Line 4), i.e., all non-converted residuals in \vec{r} fall below the desired threshold in Eq. (15). Eventually, Algo. 1 returns \vec{q} as the diffused vector of \vec{f} . Theorem IV.1 establishes the approximation accuracy guarantees of Algo. 1 and indicates that GreedyDiffuse runs in time proportional to the size of \vec{f} and $\frac{1}{(1-\alpha)\epsilon}$, but independent of the size of the input graph \mathcal{G} . This indicates that GreedyDiffuse enables the local estimation of RWR $\vec{\pi}$ and $\vec{\rho}$ if $\vec{\mathbf{1}}^{(s)}$ and $\vec{\phi}'$ are given as input, respectively. **A**

Running Example. Consider the example \mathcal{G} in Fig. 4. The input vector \vec{f} is a length-10 vector in which the first and second entries are 0.4 and 0.6. We conduct GreedyDiffuse over \mathcal{G} with restart factor $\alpha = 0.8$ and diffusion threshold $\epsilon = 0.1$. Initially, the residuals of v_1 and v_2 are 0.4 and 0.6 as in \vec{f} , while the reserves of all nodes are 0 as in Fig. 4(a). Since $\frac{\vec{r}_1}{d(v_1)} = 0.4/4 \geq \epsilon$ and $\frac{\vec{r}_2}{d(v_2)} = 0.6/3 \geq \epsilon$, GreedyDiffuse converts the $1-\alpha = 0.2$ portion of their residuals into their reserves and distributes the rest to their neighbors evenly. Specifically, nodes v_2 - v_5 receive a residual of $\frac{0.4\alpha}{d(v_1)} = 0.08$ from v_1 , respectively, while each of nodes v_1 , v_3 , and v_4 receives $\frac{0.6\alpha}{d(v_2)} = 0.16$ residual. Notably, both v_3 and v_4 have a total residual of 0.24, which satisfy $\frac{0.24}{d(v_3)} = \frac{0.24}{d(v_4)} = 0.12 \geq \epsilon$. Thus, in the second iteration, GreedyDiffuse merely performs diffusion operations on v_3 and v_4 . A residual of $0.24(1-\alpha) = 0.048$ will be converted into their reserves, and a residual of $\frac{0.24\alpha}{d(v_3)} = \frac{0.24\alpha}{d(v_4)} = 0.096$ will be transferred to v_1 and v_2 from v_3 and v_4 , respectively. The residuals at v_1 , v_2 , and v_5 are updated to 0.352, 0.272, and 0.08, respectively, leading to $\frac{0.352}{d(v_1)} = 0.088$, $\frac{0.272}{d(v_2)} = 0.0907$, $\frac{0.08}{d(v_5)} = 0.016$, all of which are less than $\epsilon = 0.1$. GreedyDiffuse then terminates and returns the reserve values as the result.

B. An Empirical Study of GreedyDiffuse

Although GreedyDiffuse enjoys favorable theoretical properties in Theorem IV.1, it suffers from slow convergence

Algorithm 2: AdaptiveDiffuse

Input: $P, \alpha, \sigma, \epsilon, \vec{f}$
Output: Diffused vector \vec{q}

- 1 $\vec{r} \leftarrow \vec{f}; \vec{q} \leftarrow \mathbf{0}; C_{tot} \leftarrow 0;$
- 2 **while** *true* **do**
- 3 Line 3 is the same as Line 3 in Algo. 1;
- 4 **if** $\frac{|\text{supp}(\vec{r})|}{|\text{supp}(\vec{q})|} > \sigma$ **and** $C_{tot} + \text{vol}(\vec{r}) < \frac{\|\vec{f}\|_1}{(1-\alpha)\epsilon}$ **then**
- 5 $C_{tot} \leftarrow C_{tot} + \text{vol}(\vec{r});$
- 6 Update \vec{q} and \vec{r} ; \triangleright Eq. (17)
- 7 **else**
- 8 Lines 8-11 are the same as Lines 4-7 in
- 9 Algo. 1;
- 12 **return** \vec{q} ;

on real graphs due to its aggressive strategy in Eq. (16). To exemplify, we evaluate the residual sum $\|\vec{r}\|_1$ at the end of each iteration in Algo. 1 when adopting greedy (Lines 5-7) and *non-greedy* operations (Eq. (17)) on *PubMed* and *ArXiv* datasets (Table III).

$$\vec{q} \leftarrow \vec{q} + (1 - \alpha)\vec{r}, \quad \vec{r} \leftarrow \alpha\vec{r}P \quad (17)$$

Distinct from the greedy way in Eq. (16), non-greedy operations in Eq. (17) directly convert and diffuse the residuals of *all* nodes in one shot in each iteration. From Fig. 5, we can observe that Algo. 1 using the greedy strategy needs $2\times$ more iterations to terminate and near $4\times$ more iterations to attain the same residual sum compared to its non-greedy variant on both datasets, leading to inferior empirical efficiency. The reason is that GreedyDiffuse always attempts to sift out a small moiety of low-degree nodes (Eq. (15)) for residual conversion and diffusion in each iteration (Line 5), making it sensitive to high-degree nodes and leaving the bulk of residual untouched. Such a way tends to trigger relentless residual accumulation and propagation among a minority of nodes, causing numerous iterations but fewer non-zero entries in \vec{q} . As reported in Table II, on real datasets on *ArXiv* and *Yelp*, the average node degrees of local clusters output by GreedyDiffuse are notably lower than the average node degrees of the entire graphs and those by the non-greedy strategy.

In contrast, non-greedy operations transform $1 - \alpha = 20\%$ of residuals into reserves in each iteration, making $\|\vec{r}\|_1$ decrease rapidly after a few iterations, e.g., $\|\vec{r}\|_1 = 0.107$ after only 10 iterations. Meanwhile, the residual is evenly distributed across more nodes, each with a small value, enabling early termination. However, due to its brute-force nature, the non-greedy strategy entails up to $O(m)$ cost in $\alpha\vec{r}P$ of each iteration in the worst case, especially on dense graphs.

C. The AdaptiveDiffuse Approach

Inspired by the preceding analysis, we propose combining greedy and non-greedy operations in an adaptive way to overcome the limitations of both, ensuring fast termination and high locality.

TABLE II: Average node degrees of local clusters ($\epsilon = 10^{-7}$).

Dataset	Global avg. degree	Greedy	Non-greedy
<i>PubMed</i>	13.77	12.49	14.39
<i>Yelp</i>	20.47	17.83	22.65

The pseudo-code of this AdaptiveDiffuse method is provided in Algo. 2, which additionally requires inputting a parameter $\sigma \in [0, 1]$ and a variable C_{tot} tracking the total cost incurred by non-greedy diffusion operations. In contrast to Algo. 1, in each iteration, after calculating \vec{r} by Eq. (15) at Line 3, Algo. 2 adaptively selects the greedy strategy (Lines 8-11) or non-greedy way (Lines 5-6) based on the following conditions. The rationale is to first deplete the residuals through non-greedy diffusion as much as possible (for faster convergence) and then disseminate the rest carefully with greedy operations (for rigorous guarantees). To be specific, AdaptiveDiffuse conducts non-greedy diffusion operations when the fraction of nodes with residues above the threshold (Eq. (15)), i.e., $|\text{supp}(\vec{r})|/|\text{supp}(\vec{q})|$, outstrips σ , and in the meantime, the total cost C_{tot} after conducting such non-greedy operations, i.e., $C_{tot} + \text{vol}(\vec{r})$, is still less than the total cost using GreedyDiffuse, i.e., $\frac{\|\vec{f}\|_1}{(1-\alpha)\epsilon}$. Notice that the smaller σ is, the more non-greedy operations will be conducted. When $\sigma = 0$, AdaptiveDiffuse prioritizes executing Lines 5-6 over Lines 8-11. Once the non-greedy (Lines 5-6) strategy is chosen, C_{tot} is increased by the volume of \vec{r} , i.e., the amount of work needed in computing $\alpha\vec{r}P$. In turn, the same theoretical properties as GreedyDiffuse can be proved in the following lemma for AdaptiveDiffuse:

Theorem IV.2. *Algo. 2 outputs a vector \vec{q} such that Eq. (14) holds $\forall v_t \in \mathcal{V}$ using $O\left(\max\left\{|\text{supp}(\vec{f})|, \frac{\|\vec{f}\|_1}{(1-\alpha)\epsilon}\right\}\right)$ time.*

In addition, Lemma IV.3 states that the support size and the volume of the vector \vec{q} returned by Algo. 2 is bounded, solely dependent on $\|\vec{f}\|_1$, α , and ϵ .

Lemma IV.3. *Let \vec{f} and \vec{q} be the input and output of Algo. 2, respectively. Then, $|\text{supp}(\vec{q})| \leq \text{vol}(\vec{q}) \leq \frac{\beta\|\vec{f}\|_1}{(1-\alpha)\epsilon}$, where $1 \leq \beta \leq 2$. In particular, when $\sigma \geq 1$, $\beta = 1$.*

V. THE LACA APPROACH

This section presents our local algorithm LACA for the estimation of the BDD vector for LGC. We first elucidate the algorithmic details of Algo. 3 for constructing TNAM \mathbf{Z} . The complete algorithmic details of LACA (Algo. 4) and related analyses are provided in Section V-B. Lastly, we conduct an in-depth theoretical analysis to unveil the connection between LACA and GNNs [38].

A. Construction of TNAM \mathbf{Z}

Basic Idea. To realize the idea of transforming $s(v_i, v_j)$ into $\vec{z}^{(i)} \cdot \vec{z}^{(j)}$ (Eq. (10)), the key is to find length- k vectors $\vec{y}^{(i)} \forall v_i \in \mathcal{V}$ (i.e., an $n \times k$ matrix \mathbf{Y}) such that $f(v_i, v_j) = \vec{y}^{(i)} \cdot \vec{y}^{(j)}$. Accordingly, Eq. (1) can be rewritten as

$$s(v_i, v_j) = \frac{\vec{y}^{(i)} \cdot \vec{y}^{(j)}}{\sqrt{\vec{y}^{(i)} \cdot \vec{y}^*} \cdot \sqrt{\vec{y}^{(j)} \cdot \vec{y}^*}} = \vec{z}^{(i)} \cdot \vec{z}^{(j)}, \quad \text{where}$$

Algorithm 3: TNAM Construction

Input: Attribute matrix \mathbf{X} , function $f(\cdot, \cdot)$, and dimension k
Output: The TNAM \mathbf{Z}

- 1 $\mathbf{U}, \mathbf{\Lambda}, \mathbf{V} \leftarrow k\text{-SVD}(\mathbf{X})$;
- 2 **switch** $f(\cdot, \cdot)$ **do**
- 3 **case** *cosine similarity function* **do**
- 4 $\mathbf{Y} \leftarrow \mathbf{U}\mathbf{\Lambda}$;
- 5 **case** *exponential cosine similarity function* **do**
- 6 Sample a Gaussian matrix $\mathbf{G} \sim \mathcal{N}(0, 1)^{k \times k}$;
- 7 $\mathbf{Q} \leftarrow \text{QRDecomposition}(\mathbf{G})$;
- 8 Sample diagonal matrix $\Sigma_{ii} \sim \chi(k)$
 $\forall i \in \{1, \dots, k\}$;
- 9 Compute \mathbf{Y} ; ▷ Eq. (19)
- 10 Compute $\vec{\mathbf{y}}^*$; ▷ Eq. (18)
- 11 **for** $v_i \in \mathcal{V}$ **do** Compute $\vec{\mathbf{z}}^{(i)}$; ▷ Eq. (18)
- 12 **return** \mathbf{Z}

$$\vec{\mathbf{y}}^* = \sum_{v_\ell \in \mathcal{V}} \vec{\mathbf{y}}^{(\ell)} \text{ and } \vec{\mathbf{z}}^{(i)} = \vec{\mathbf{y}}^{(i)} / \sqrt{\vec{\mathbf{y}}^{(i)} \cdot \vec{\mathbf{y}}^*}. \quad (18)$$

Recall that the SNAS metrics in Section II-B are defined upon the dot product $\vec{\mathbf{x}}^{(i)} \cdot \vec{\mathbf{x}}^{(j)} \forall v_i, v_j \in \mathcal{V}$. Let $\mathbf{U} \in \mathbb{R}^{n \times k}$ and diagonal matrix $\mathbf{\Lambda} \in \mathbb{R}^{k \times k}$ consist of the top- k left singular vectors and top- k singular values of \mathbf{X} , respectively. Lemma V.1 connotes that $\mathbf{U}\mathbf{\Lambda}$ can be used as the k -dimensional approximation of \mathbf{X} for the construction of \mathbf{Y} .

Lemma V.1. *Let λ_{k+1} be the $(k+1)$ -th largest singular value of \mathbf{X} . Then, $\|(\mathbf{U}\mathbf{\Lambda}) \cdot (\mathbf{U}\mathbf{\Lambda})^\top - \mathbf{X}\mathbf{X}^\top\|_2 \leq \lambda_{k+1}^2$.*

Details. In Algo. 3, we describe the pseudo-code for constructing vectors $\vec{\mathbf{y}}^{(i)}$ and $\vec{\mathbf{z}}^{(i)}$ for each node $v_i \in \mathcal{V}$ based on the input node attribute matrix \mathbf{X} , the metric functions $f(\cdot, \cdot)$ in Section II-B, and a small integer $k \ll d$ (typically 32) to cope with the high-dimension d of \mathbf{X} . That is, Algo. 3 first applies a *k-truncated singular value decomposition* (k -SVD) [34] over \mathbf{X} to obtain its top- k left and right singular vectors \mathbf{U} , \mathbf{V} , and the diagonal singular value matrix $\mathbf{\Lambda}$ (Line 1). $\mathbf{U}\mathbf{\Lambda}$ then substitutes \mathbf{X} for subsequent generation of vectors $\vec{\mathbf{y}}^{(i)} \forall v_i \in \mathcal{V}$. When $f(\cdot, \cdot)$ is the cosine similarity function, it is straightforward to get $\mathbf{Y} = \mathbf{U}\mathbf{\Lambda}$ (Lines 3-4).

However, when $f(\cdot, \cdot)$ is the exponential cosine similarity function (Eq. (3)), constructing $\vec{\mathbf{y}}^{(i)}$ exactly involves the materialization of $f(v_i, v_j)$ for all node pairs in $\mathcal{V} \times \mathcal{V}$ and a matrix factorization, which is prohibitive for large graphs. As a workaround, we capitalize on the *orthogonal random features* [35] to create estimators $\vec{\mathbf{y}}^{(i)} \forall v_i \in \mathcal{V}$ such that $\vec{\mathbf{y}}^{(i)} \cdot \vec{\mathbf{y}}^{(j)} \approx f(v_i, v_j) \forall v_i, v_j \in \mathcal{V}$.

More concretely, Algo. 3 first randomly generates a $k \times k$ random Gaussian matrix \mathbf{G} with every entry sampled from the standard normal distribution independently at Line 6, followed by a QR decomposition of \mathbf{G} at Line 7. This step produces a uniformly distributed random orthogonal matrix $\mathbf{Q} \in \mathbb{R}^{k \times k}$ [44]. Algo. 3 further builds a $k \times k$ diagonal matrix

Algorithm 4: LACA

Input: $\mathcal{G} = (\mathcal{V}, \mathcal{E})$, TNAM \mathbf{Z} , seed node v_s , restart factor α , parameter σ , diffusion threshold ϵ
Output: Approximate BDD vector $\vec{\rho}'$

- /* Step 1: Estimate RWR vector $\vec{\pi}'$ */
- 1 Create a unit vector $\vec{\mathbf{1}}^{(s)} \in \mathbb{R}^n$;
- 2 $\vec{\pi}' \leftarrow \text{AdaptiveDiffuse}(\mathbf{P}, \alpha, \sigma, \epsilon, \vec{\mathbf{1}}^{(s)})$;
- /* Step 2: Compute RWR-SNAS vector $\vec{\phi}'$ */
- 3 Compute $\vec{\psi}$; ▷ Eq. (12)
- 4 **for** $i \in \text{supp}(\vec{\pi}')$ **do** Compute $\vec{\phi}'_i$; ▷ Eq. (13)
- /* Step 3: Estimate BDD vector $\vec{\rho}'$ */
- 5 $\vec{\rho}' \leftarrow \text{AdaptiveDiffuse}(\mathbf{P}, \alpha, \sigma, \epsilon \cdot \|\vec{\phi}'\|_1, \vec{\phi}')$
- 6 **for** $i \in \text{supp}(\vec{\rho}')$ **do** $\vec{\rho}'_i \leftarrow \frac{\vec{\rho}'_i}{d(v_i)}$
- 7 **return** $\vec{\rho}'$

Σ with diagonal entries sampled i.i.d. from the χ -distribution with k degrees of freedom (Line 8), enforcing the norms of the rows of $\Sigma\mathbf{Q}$ and \mathbf{G} identically distributed. Based thereon, we construct matrix \mathbf{Y} at Line 9 as follows:

$$\mathbf{Y} \leftarrow \sqrt{\frac{2 \exp(1/\delta)}{k}} \cdot \sin(\widehat{\mathbf{Y}}) \parallel \cos(\widehat{\mathbf{Y}}), \quad (19)$$

where $\widehat{\mathbf{Y}} \leftarrow \frac{1}{\delta} \mathbf{U}\mathbf{\Lambda}\Sigma\mathbf{Q}$ and \parallel stands for a horizontal concatenation of two matrices. Theorem V.2 indicates that $\vec{\mathbf{y}}^{(i)} \cdot \vec{\mathbf{y}}^{(j)}$ is an *unbiased* estimator of $f(v_i, v_j)$ for any node pair $(v_i, v_j) \in \mathcal{V} \times \mathcal{V}$.

Theorem V.2. $\mathbb{E}[\vec{\mathbf{y}}^{(i)} \cdot \vec{\mathbf{y}}^{(j)}] = f(v_i, v_j)$ in Eq. (3).

After computing vector $\vec{\mathbf{y}}^{(i)}$ for each node $v_i \in \mathcal{V}$, Algo. 3 first computes the sum of these vectors, i.e., $\vec{\mathbf{y}}^*$, and finally constructs $\vec{\mathbf{z}}^{(i)}$ for each node $v_i \in \mathcal{V}$ by Eq. (18) (Lines 10-11). The total processing cost entailed by Algo. 3 is linear to the size of the input node attribute matrix \mathbf{X} , as proved in the following lemma:

Lemma V.3. *The runtime cost of Algo. 3 is $O(nd)$.*

B. Complete Algorithm and Analysis

In Algo. 4, we present the complete pseudo-code of LACA, which takes as input the attributed graph \mathcal{G} , the TNAM \mathbf{Z} obtained in the preprocessing stage, seed node v_s , diffusion threshold ϵ , and parameters α and σ . In the first place, Algo. 4 invokes AdaptiveDiffuse (Algo. 2) with a unit vector $\vec{\mathbf{1}}^{(s)}$ as input, which has value 1 at entry s and 0 everywhere else (Lines 1-2). By Lemma IV.3, the support size $|\text{supp}(\vec{\pi}')|$ of the returned RWR vector $\vec{\pi}'$ is bounded by $O\left(\frac{1}{(1-\alpha)\epsilon}\right)$. Next, $\vec{\pi}'$ is used for producing vector $\vec{\psi} \leftarrow \vec{\pi}' \cdot \mathbf{Z}$ at Line 3 and subsequently the RWR-SNAS vector $\vec{\phi}'$ at Line 4. In particular, in lieu of computing $\vec{\phi}'_i$ for each node $v_i \in \mathcal{V}$ by Eq. (13), LACA merely accounts for nodes with non-zero entries in vector $\vec{\pi}'$, i.e., $i \in \text{supp}(\vec{\pi}')$, whereby the number of non-zero entries in $\vec{\phi}'$ can be guaranteed to be bounded by

$O\left(\frac{1}{(1-\alpha)\epsilon}\right)$. After that, LACA starts to diffuse the RWR-SNAS vector $\vec{\phi}'$ over graph \mathcal{G} using the AdaptiveDiffuse with diffusion threshold $\epsilon \cdot \|\vec{\phi}'\|_1$, and parameters α and σ (Line 5). Let $\vec{\rho}'$ be the output of the above diffusion process. LACA then gives $\vec{\rho}'$ a final touch by dividing each non-zero entry $\vec{\rho}'_i$ in $\vec{\rho}'$ by $\frac{1}{d(v_i)}$ (Line 6) and returns $\vec{\rho}'$ as the approximate BDD vector at Line 7. On the basis of Theorem IV.2, we can establish the accuracy guarantee of LACA as follows:

Theorem V.4. *When the TNAM \mathbf{Z} and SNAS $s(v_i, v_j) \forall v_i, v_j \in \mathcal{V}$ satisfy Eq. (10), $\vec{\rho}'$ output by Algo. 4 ensures $\forall v_t \in \mathcal{V}$*

$$0 \leq \vec{\rho}_t - \vec{\rho}'_t \leq \left(1 + \sum_{v_i \in \mathcal{V}} d(v_i) \cdot \max_{v_j \in \mathcal{V}} s(v_i, v_j)\right) \cdot \epsilon.$$

Volume and Complexity Analysis. Recall that $\vec{\rho}'$ is obtained by calling AdaptiveDiffuse with $\vec{f} = \vec{\phi}'$ and diffusion threshold $\epsilon \cdot \|\vec{\phi}'\|_1$. Both the support size $|\text{supp}(\vec{\rho}')|$ and volume $\text{vol}(\vec{\rho}')$ of $\vec{\rho}'$ are therefore bounded by $O\left(\frac{1}{(1-\alpha)\epsilon}\right)$ using Lemma IV.3.

Next, we analyze the time complexity of LACA. First, Line 2 invokes Algo. 1 with a one-hot vector $\vec{\mathbf{1}}^{(s)}$, i.e., $\|\vec{\mathbf{1}}^{(s)}\|_1 = 1$, entailing $O\left(\frac{1}{(1-\alpha)\epsilon}\right)$ time as per Theorem IV.2. The cost of Lines 3 and 4 is dependent on the number of non-zero elements in vector $\vec{\pi}'$, i.e., $|\text{supp}(\vec{\pi}')|$, and the dimension k of \mathbf{Z} , which is $O\left(\frac{k}{(1-\alpha)\epsilon}\right)$ time by Lemma IV.3. Analogously, we can derive that the computational complexities of Lines 6-7 are $O\left(\max\left\{|\text{supp}(\vec{\phi}')|, \frac{\|\vec{\phi}'\|_1}{(1-\alpha)\epsilon \cdot \|\vec{\phi}'\|_1}\right\}\right) = O\left(\frac{1}{(1-\alpha)\epsilon}\right)$. Overall, the time complexity of LACA is $O\left(\frac{k}{(1-\alpha)\epsilon}\right)$, which equals $O(1/\epsilon)$ when α and k are regarded as constants and is linear to the volume of its output $\vec{\rho}'$.

C. Theoretical Connection to GNNs

Recent studies [45], [46] demystify that learning node representations \mathbf{H} via existing canonical GNN architectures can be characterized by a graph smoothing process in Definition V.5.

Definition V.5 (Graph Signal Denoising [45]). Let \mathbf{L} be the normalized Laplacian matrix of \mathcal{G} and $\mathbf{H}^\circ \in \mathbb{R}^{n \times k}$ be a feature matrix. The graph signal denoising is to optimize \mathbf{H} :

$$\arg \min_{\mathbf{H}} (1 - \alpha) \|\mathbf{H} - \mathbf{H}^\circ\|_F^2 + \alpha \cdot \text{trace}(\mathbf{H}^\top \mathbf{L} \mathbf{H}), \quad (20)$$

where $\|\cdot\|_F$ stands for the matrix Frobenius norm.

The fitting term $\|\mathbf{H} - \mathbf{H}^\circ\|_F^2$ in Eq. (20) seeks to make the final node representations \mathbf{H} close to the initial feature matrix \mathbf{H}° , while the graph Laplacian regularization term $\text{trace}(\mathbf{H}^\top \mathbf{L} \mathbf{H})$ forces learned representations of two adjacent nodes over \mathcal{G} to be similar. The hyperparameter $\alpha \in [0, 1]$ controls the smoothness of \mathbf{H} through graph regularization.

Lemma V.6. *The closed-form solution to Eq. (20) is $\mathbf{H} = \sum_{\ell=0}^{\infty} (1 - \alpha) \alpha^\ell \tilde{\mathbf{A}}^\ell \mathbf{H}^\circ$, where $\tilde{\mathbf{A}} = \mathbf{D}^{-\frac{1}{2}} \mathbf{A} \mathbf{D}^{-\frac{1}{2}}$.*

By applying the gradient descent to solve Eq. (20), Lemma V.6 states that the final representation $\vec{h}^{(i)}$ of

TABLE III: Statistics of Datasets.

Dataset	n	m	m/n	d	$ \overline{\mathcal{Y}}_s $
<i>Cora</i> [48]	2,708	5,429	2.01	1,433	488
<i>PubMed</i> [48]	19,717	44,338	2.25	500	7,026
<i>BlogCL</i> [49]	5,196	343,486	66.11	8,189	869
<i>Flickr</i> [50]	7,575	479,476	63.30	12,047	846
<i>ArXiv</i> [51]	169,343	1,166,243	6.89	128	12,828
<i>Yelp</i> [52]	716,847	7,335,833	10.23	300	476,555
<i>Reddit</i> [52]	232,965	11,606,919	49.82	602	9,418
<i>Amazon2M</i> [53]	2,449,029	61,859,140	25.26	100	260,129

any node $v_i \in \mathcal{V}$ can be formulated as $\vec{h}^{(i)} = \sum_{\ell=0}^{\infty} (1 - \alpha) \alpha^\ell \tilde{\mathbf{A}}^\ell \vec{h}^{\circ(i)}$, where the normalized adjacency matrix $\tilde{\mathbf{A}}$ can also be replaced by the transition matrix \mathbf{P} in popular GNN models [47].

If we let TNAM \mathbf{Z} be the initial feature matrix \mathbf{H}° input to GNN models, the eventual smoothed node representations (a.k.a. embeddings) are $\mathbf{H} = \sum_{\ell=0}^{\infty} (1 - \alpha) \alpha^\ell \mathbf{P}^\ell \mathbf{Z}$. When Eq. (10) holds, combining Eq. (5) and Eq. (6) leads to $\forall v_t \in \mathcal{V}, \vec{\rho}_t = \vec{h}^{(s)} \cdot \vec{h}^{(t)}$, implying that $\vec{\rho}'$ output by LACA essentially approximates $\vec{h}^{(s)} \cdot \mathbf{H}^\top$. In this view, our LGC task that extracts a local cluster \mathcal{C}_s from \mathcal{G} based on BDD values is equivalent to identifying the K -NN ($K = |\mathcal{C}_s|$) of $\vec{h}^{(s)}$ among n GNN-like embeddings $\{\vec{h}^{(t)} | v_i \in \mathcal{V}\}$. Distinctly, our LACA approach fulfills this goal without explicitly materializing the GNN-like embeddings \mathbf{H} and incurring the $\tilde{O}(n)$ cost by the K -NN search, but undergoes a local exploration of \mathcal{G} in time linear to the volume of \mathcal{C}_s , regardless of n and m .

VI. EXPERIMENTS

This section experimentally evaluates our proposed LACA against 17 alternative solutions to LGC on 8 real datasets, in terms of both local clustering quality and efficiency. All experiments are conducted on a Linux machine powered by Intel Xeon(R) Gold 6330 2.00GHz CPUs and 2TB memory. Due to space limits, additional experimental results regarding the parameter analysis, ablation study, scalability tests, and the LGC quality of LACA on non-attributed graphs are deferred to Appendix B. For reproducibility, the source code, datasets, and detailed parameter settings are available at <https://github.com/HaoranZ99/laca>.

A. Experimental Setup

Datasets. Table III lists the statistics of the datasets used in the experiments. The numbers of nodes, edges, and distinct attributes of the graph data are denoted as n , m , and d , respectively. $|\overline{\mathcal{Y}}_s|$ stands for the average size of the ground-truth local clusters of all nodes in the graph. *Cora*, *PubMed* [48], and *ArXiv* [51] are citation networks, where nodes and edges represent publications and citation links among them, respectively. The attributes of each node are bag-of-words embeddings of the corresponding publication. The ground-truth local cluster \mathcal{Y}_s of each publication contains the publications in its same subject areas. *BlogCL* [49] and *Flickr* [50] are social networks extracted from the BlogCatalog and Flickr websites, respectively. \mathcal{Y}_s of each user $v_s \in \mathcal{V}$ includes users who are in the same topic categories or interest groups. *Yelp* and *Reddit*

TABLE IV: Evaluated methods.

Method	Category	Preprocessing Cost	Online Cost
PR-Nibble [15]	Local Graph Clustering	-	$\tilde{O}\left(\frac{1}{\epsilon}\right)$
APR-Nibble		$O(md)$	
HK-Relax [16]		-	$\tilde{O}\left(\frac{\log(1/\epsilon)}{\epsilon}\right)$
CRD [20]		-	$O\left(\frac{1}{\epsilon}\right)$
p -Norm FD [21]		-	$O\left(\frac{\max_{v_i \in \mathcal{V}} d(v_i)^2}{\epsilon}\right)$
WFD [33]		$O(md)$	
Jaccard [54]	Link Similarity	-	$\tilde{O}(n)$
Adamic-Adar [54]		-	
Common-Nbrs [54]		-	
SimRank [55]		-	
SimAttr [56], [57]	Attribute Similarity	-	$\tilde{O}(nd)$
AttriRank [58]		$O(nd^2 + m)$	$\tilde{O}(n)$
Node2Vec [59]	Node Embedding	$O(n)$	$\tilde{O}(n)$
SAGE [38]		$O(nd^2)$	
PANE [60], [61]		$O((m+n) \cdot d)$	
CFANE [62]		$O((m+n) \cdot d)$	
LACA		$O(nd)$	

datasets are collected from in [52]. *Yelp* contains friendships between *Yelp* users, those who have been to the same types of business constitute local clusters. *Reddit* connects online posts if the same user comments on both and the communities of posts are used as local clusters. *Amazon2M* [53] is a co-purchasing network of Amazon products wherein each node corresponds to a product and each edge represents that two products are purchased together. The ground-truth local clusters are generated based on the categories of products.

Competitors. We dub our LACA algorithms using metric functions cosine similarity and exponential cosine similarity as LACA (C) and LACA (E), respectively. We experimentally compare LACA (C) and LACA (E) against 17 methods adopted for LGC, which can be categorized into four groups:

- 1) LGC-based methods: PR-Nibble [15], APR-Nibble, HK-Relax [16], CRD [20], p -Norm FD [21], and WFD [33];
- 2) Link Similarity-based methods: Jaccard [54], Adamic-Adar [54], Common-Nbrs [54], and SimRank [55];
- 3) Attribute Similarity-based methods: SimAttr (C) [56], SimAttr (E) [57], and AttriRank [58];
- 4) Network Embedding-based methods: Node2Vec [59], SAGE [38], PANE [60], [61], and CFANE [62].

Amid LGC-based approaches, PR-Nibble [15], APR-Nibble, and HK-Relax [16] are based on random walk graph diffusion, while CRD [20], p -Norm FD [21], and WFD [33] leverages maximum flow algorithms, all of which are *local* algorithms. APR-Nibble is a variant of PR-Nibble wherein edges are weighted by the Gaussian kernel of their endpoints’ attribute vectors, similar to WFD [33]. Groups 2)-4) comprise all *global* methods. Link similarity-based and attribute similarity-based methods calculate the link-based and attribute-based similarities between the seed node and *all* nodes, respectively. The local clusters are then generated by sorting all nodes according to the similarity scores. The fourth category of methods first encodes all nodes in the

input graph into low-dimensional embedding vectors and then obtains the local clusters for given seed nodes through the K -NN, spectral clustering (SC), or DBSCAN over the embedding vectors. Particularly, SAGE [38], PANE [61], and CFANE [62] incorporate both topology and attribute semantics into the embeddings, whereas Node2Vec [59] disregard nodal attributes. Table IV summarizes the preprocessing cost and average complexity of these algorithms for generating local clusters.

Implementations and Parameter Settings. For PR-Nibble, CRD, and APR-Nibble, we use their implementations provided by [63]. We also employ the well-known NetworkX [64] package for the computation of link similarities of nodes, including Jaccard, Adamic-Adar, Common-Nbrs, and SimRank. As for other competitors, we obtain their source codes from the respective authors. All competitors are implemented in Python, except p -Norm FD and WFD, which have been implemented in Julia. For a fair comparison, we run grid searches for parameters and report the results corresponding to the best precision for LGC-based methods, LACA (C), and LACA (E). The parameters in global methods are set as suggested in their respective papers. On each dataset, we randomly select 500 seed nodes S from the graph for LGC tasks. All evaluation results reported in the experiments are averaged over seed nodes in S .

B. Quality Evaluation

1) **Precision:** In this set of experiments, we empirically evaluate the average precisions of the local clusters returned by LACA (C), LACA (E), and the 17 competitors in four categories, respectively, based on the ground-truth local clusters. More concretely, for each seed node v_s in S , we run all the evaluated methods such that the predicted local cluster \mathcal{C}_s satisfies $|\mathcal{C}_s| = |\mathcal{Y}_s|$ and calculate the precision as $|\mathcal{C}_s \cap \mathcal{Y}_s|/|\mathcal{C}_s|$. Table V reports the average precision scores achieved by all the evaluated approaches on 8 datasets. The best results among all methods are highlighted in bold, and the best performance by the competitors is underlined. We exclude any method with a preprocessing time exceeding 3 days or an average running time for LGC over 2 hours.

Overall, our methods LACA (C) and LACA (E) achieve the top-2 best average ranks in terms of precision on all datasets. Specifically, on small datasets *Cora*, *PubMed*, *BlogCL*, and *Flickr*, LACA (C) and LACA (E) consistently outperform all the competitors, often by a large margin. For instance, on *Cora* and *Flickr*, compared to the state-of-the-art baseline CFANE and PANE, LACA (C) is able to take a lead by 6.1% and 11.5%, respectively. Similar observations can be made on the medium-sized graph *ArXiv* with over one million edges and the largest dataset *Amazon2M* with 61.9 million edges, where both LACA (C) or LACA (E) outperforms the best competitor by a margin of up to 2.6% and 1.8%, respectively. Over other large graphs *Yelp* and *Reddit*, LACA (C) and LACA (E) also obtain comparable or superior prediction precision. Note that on *Yelp* LACA is slightly inferior to SimAttr (C) and SimAttr (E), with merely a 0.4% decline in precision, but significantly

TABLE V: The average precision evaluated with ground-truth. Best is **bolded** and best baseline underlined.

Method		Cora [48]	PubMed [48]	BlogCL [49]	Flickr [50]	ArXiv [52]	Yelp [51]	Reddit [51]	Amazon2M [53]	Rank
Local Graph Clustering	PR-Nibble [15]	0.413	0.481	0.263	0.198	0.299	0.214	0.651	0.364	9.25
	APR-Nibble	0.396	0.479	0.252	0.173	0.282	0.093	0.435	0.129	13.13
	HK-Relax [16]	0.477	0.476	0.284	0.219	<u>0.351</u>	0.214	0.751	0.116	8.63
	CRD [20]	0.149	0.112	0.236	0.192	0.166	0.098	0.641	0.072	16.38
	p -Norm FD [21]	0.263	0.131	0.159	0.132	0.225	0.034	<u>0.806</u>	0.441	16.5
	WFD [33]	0.298	0.17	0.181	0.133	0.253	0.043	<u>0.589</u>	<u>0.503</u>	15.63
Link Similarity	Jaccard [54]	0.231	0.358	0.282	0.209	0.116	0.662	0.343	0.142	13.13
	Adamic-Adar [54]	0.231	0.358	0.265	0.163	0.117	0.662	0.33	0.142	15
	Common-Nbrs [54]	0.231	0.358	0.259	0.156	0.115	0.662	0.318	0.142	16
	SimRank [55]	0.436	0.519	0.273	0.186	-	-	-	-	9.25
Attribute Similarity	SimAttr (C) [56]	0.288	0.469	0.306	0.182	0.154	0.758	0.035	0.194	10.88
	SimAttr (E) [57]	0.288	0.469	0.306	0.182	0.154	0.758	0.035	0.194	10.88
	AttriRank [58]	0.181	0.363	0.184	0.124	0.076	0.666	0.047	0.122	18.25
Network Embedding	Node2Vec (K -NN)	0.181	0.363	0.167	0.111	0.074	0.665	-	-	20.5
	Node2Vec (SC)	0.41	0.488	0.263	0.182	-	-	-	-	12.25
	Node2Vec (DBSCAN)	0.419	0.488	0.263	0.182	0.316	0.679	-	-	9.5
	SAGE (K -NN)	0.423	0.434	0.209	0.143	-	-	-	-	18
	SAGE (SC)	0.403	0.399	0.226	0.155	-	-	-	-	18.5
	SAGE (DBSCAN)	0.326	0.359	0.226	0.155	-	-	-	-	20
	CFANE (K -NN)	<u>0.495</u>	<u>0.531</u>	<u>0.505</u>	0.2	-	-	-	-	4
	CFANE (SC)	0.494	<u>0.531</u>	<u>0.505</u>	0.198	-	-	-	-	4.5
	CFANE (DBSCAN)	0.383	0.44	0.36	0.164	-	-	-	-	14.25
	PANE (K -NN)	0.445	0.497	0.456	<u>0.332</u>	0.147	0.708	0.263	0.197	6.88
	PANE (SC)	0.445	0.497	0.456	<u>0.332</u>	-	-	-	-	5
	PANE (DBSCAN)	0.422	0.477	0.267	0.264	0.145	0.635	0.232	0.177	10.88
Ours	LACA (C)	0.556	0.552	0.51	0.447	0.377	0.754	0.808	0.465	1.63
	LACA (E)	0.552	0.555	0.493	0.39	0.377	0.739	0.808	0.521	2

Legend for Figure 6: LACA (C) (orange circle), LACA (E) (green star), LACA (w/o SNAS) (red diamond), PR-Nibble (blue square), HK-Relax (purple triangle), APR-Nibble (cyan plus).

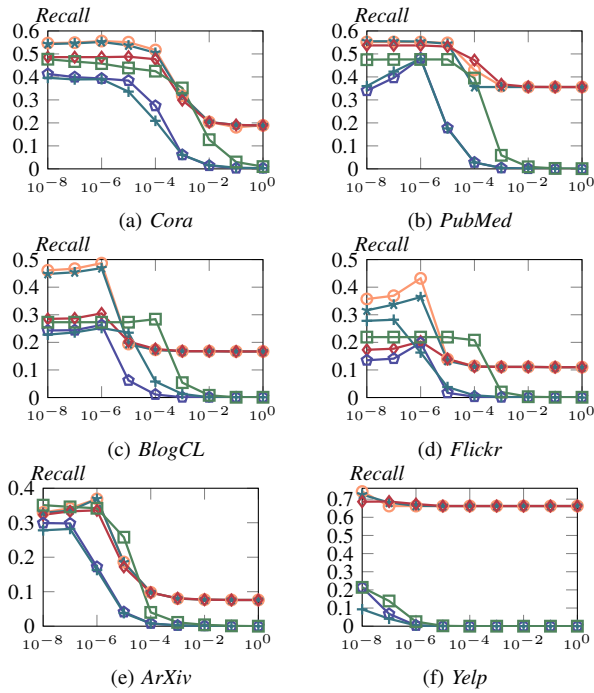


Fig. 6: Recall when varying ϵ .

dominates other competitors by a substantial margin of at least 4.6%. The reason is that the ground-truth clusters in the *Yelp* dataset are more relevant to node attributes than graph structures. LACA is the only LGC solution that can handle such graphs without downgrading the precision, exhibiting the effectiveness of our algorithmic designs in combining attribute and structure information. This also underlines a limitation

of LACA on graph datasets with high-quality attributes but substantial poor/corrupted structures, e.g., heterophilic graphs. In addition, we can observe that LACA (C) attains comparable or superior performance to LACA (E) in most datasets. The only exception is on *Amazon2M*, where LACA (E) obtains an improvement of 5.9% over LACA (C).

2) **Recall when varying ϵ :** This set of experiments studies the effectiveness of LACA and other LGC-based methods in recovering the ground-truth local clusters when the sizes of their predicted ones (i.e., runtime budget) are varied. For a fair comparison, we only compare LACA (C) and LACA (E) with graph diffusion-based baselines PR-Nibble, APR-Nibble, and HK-Relax as the sizes of their output local clusters can be controlled by diffusion threshold ϵ and are bounded by $O(1/\epsilon)$. We additionally include an ablated version of LACA, dubbed as LACA (w/o SNAS), for comparison, which disables attribute information in LACA. For all evaluated algorithms, we vary the size of the output local clusters by decreasing ϵ from 1.0 to 10^{-8} . For each seed node $v_s \in \mathcal{S}$, given the predicted local cluster C_s , we compute the recall by $|C_s \cap \mathcal{Y}_s|/|\mathcal{Y}_s|$. Intuitively, the smaller ϵ is, the higher the recall should be. Fig. 6 depicts the average recall scores by all six methods when varying ϵ on six datasets. The x -axis and y -axis represent ϵ and the average recall, respectively.

From Fig. 6, we can make the following observations. In most cases, both LACA (C) and LACA (E) consistently outperform other methods under the same diffusion thresholds ϵ . In particular, on all datasets, the superiority of LACA (C) and LACA (E) is pronounced when $\epsilon \geq 10^{-3}$, indicating that LACA is effective and favorable when the budget for the sizes of local clusters and costs is low (e.g., only a small portion of the graph is allowed to be explored). When $\epsilon \leq 10^{-6}$, we can make qualitatively analogous observations on all datasets

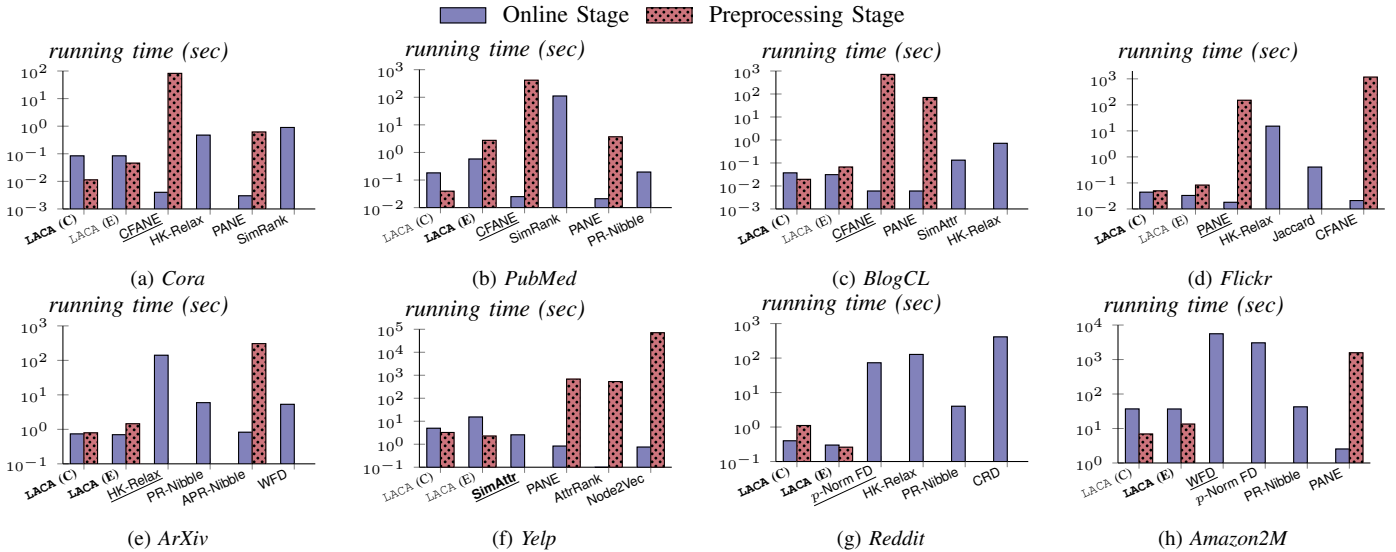


Fig. 7: Running times. Best method and competitor (in terms of precision) are bolded and underlined, respectively.

except *ArXiv*, where LACA (C), LACA (E), LACA (w/o SNAS), and HK-Relax perform comparably. Notice that on *BlogCL*, *Flickr*, and *ArXiv*, Hk-Relax outmatches LACA (C) and LACA (E) when ϵ is roughly 10^{-4} or 10^{-5} . The reason is that HK-Relax produces \mathcal{C}_s with larger sizes than that by LACA under the same ϵ owing to its higher running time (Table IV). Furthermore, it can be seen that LACA (w/o SNAS) obtains similar results to LACA (C) and LACA (E) when ϵ is large and inferior ones when ϵ is small, which are still superior to those by other methods on most datasets. *This phenomenon implies that (i) our BDD (even without attributes) is more effective than existing graph diffusion metrics (personalized PageRank [41] and heat kernel PageRank [65]) in exploiting topological features for LGC, and (ii) the SNAS (attribute information) in LACA is crucial for identifying the nodes in \mathcal{C}_s that are far from the seed.*

Further, in Appendix B, we evaluate the average external connectivity (i.e., conductance) and attribute variance (a.k.a. WCSS) of nodes in local clusters output by all methods. We also showcase that our LACA’s framework remains effective on non-attributed graphs in Appendix B.

C. Efficiency Evaluation

For ease of comparison, on each dataset, we assess the empirical efficiency of LACA (C) and LACA (E) only against the methods that yield the top-4 best results among all competitors in terms of precision (Table V). In Fig. 7, we show the running times (measured in wall-clock time) required by the preprocessing phase and the online phase (i.e., the procedure generating a local cluster for a single seed node) of each evaluated approach. The y -axis represents the running time in seconds on a log scale.

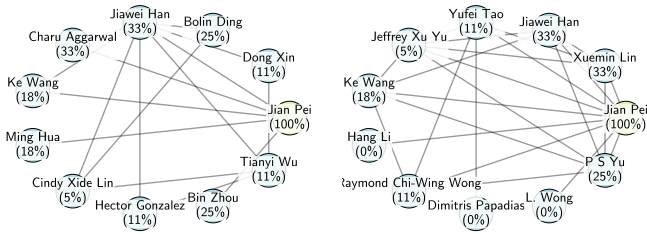
The first observation we can make from Fig. 7 is that on small datasets *Cora*, *PubMed*, *BlogCL*, and *Flickr*, LACA (C), LACA (E) and the-state-of-the-art solutions (CFANE or PANE) are highly fast in the online stage, all of which take less than

0.1 seconds to finish a LGC task on average. However, CFANE and PANE obtain such a high online efficiency at the cost of up to 19.4 and 2.5 minutes for constructing node embeddings of all nodes in the preprocessing, whereas LACA (C) and LACA (E) require at most 2.8 seconds.

On larger graphs *ArXiv*, *Reddit*, and *Amazon2M* comprising millions or tens of millions of edges, CFANE fails to report the results within 3 days and LGC-based methods HK-Relax, p -Norm FD and WFD are the state-of-the-art solutions. On such datasets, LACA (C) and LACA (E) are able to gain a significant speedup of $196\times$, $209\times$, and $152\times$, respectively, in the online stage on average. Note that the total preprocessing costs of LACA (C) and LACA (E) are still insignificant, which often take a few seconds, even less than the average cost for a single LGC task. For instance, on the largest dataset *Amazon2M*, with 62 million edges, LACA (E) attains a precision of 0.521 using an average of 36.7 seconds for Algo. 4 (online stage) and 13.4 seconds for TNAM construction (preprocessing stage). In comparison, the best competitor WFD consumes 92.9 minutes to get a precision of 0.503. The empirical observations are consistent with the theoretical evidence that HK-Relax, p -Norm FD and WFD have worse asymptotic complexities than LACA as in Table IV. On *Yelp*, where the best methods SimAttr (C) and SimAttr (E) are simply based on attributes, LACA (C) and LACA (E) have comparable prediction precision using slightly higher running time. In summary, our LACA methods can achieve significantly higher efficiency for LGC on most attributed graphs with various volumes and meanwhile yield state-of-the-art result quality.

D. Real-world Example

Our proposed adaptive local clustering method can be applied to real-world scenarios, including the following three representative applications: game club recommendation [2], social network analysis (e.g., Twitter community



(a) Run LACA on “Jian Pei” (b) Run PR-Nibble on “Jian Pei”

Fig. 8: A real-world scenario on an academic network.

detection) [17], [66], [67], and academic collaboration networks [68]. A specific validation is conducted using the academic collaboration graph from the AMiner Coauthor dataset [69], which contains 1.7M scholars with co-authorships and keyword-based research interests. Applying LACA starting from the seed scholar “Jian Pei”, we identified 10 scholars with both strong co-authorship ties and aligned research interests, as shown in Fig. 8(a). This group includes direct co-authors such as “Jiawei Han” (similarity: 33%) and “Charu Aggarwal” (33%) as well as a subgroup centered around “Jiawei Han” (e.g., “Bolin Ding” (25%)). In contrast, PR-Nibble—an LGC baseline—selected three scholars (e.g., “Hang Li,” “Dimitris Papadias”) with 0% similarity despite direct co-authorships (Fig. 8(b)). This stark difference (3/10 zero-similarity nodes in PR-Nibble vs. 0/10 in ours) demonstrates how ignoring attributes, as in LGC methods, risks recommending collaborators with mismatched expertise, even when strong structural ties exist.

VII. RELATED WORK

A. Local Graph Clustering

Local graph clustering (LGC) aims to find a high-quality local cluster without traversing the whole graph. The common characteristic of such methods is to optimize the conductance of the local cluster so that the target cluster is internally tightly connected while loosely connected to nodes outside the target cluster. Literature on LGC methods commonly distinguishes between two main types: random walk-based and flow-based methods (see [70] for a systematic survey). Among random walk-based methods [2], [14]–[17], [24], [26], [27], [32], [71], Nibble [14], PR-Nibble [15] and subsequent [2], [24], [26], [27], [32], [71] are proposed to perform local clustering via approximate personalized PageRank. Similarly, [16], [17] discuss the use of approximate heat kernel, including an LGC approach HK-Relax [16]. The flow-based methods include [20]–[22], [33], [72]. CRD [20] converts capacity diffusion into a maximum-flow problem. p -Norm FD [21] incorporates spectral and maximum-flow-based methods by choosing different p values.

These methods usually provide theoretical guarantees on running time and approximation quality. However, these guarantees may not be useful in practical efficacy. Considering this, recent works [31]–[33], [72] utilized additional graph resources besides connectivity. More specifically, WFD [33] adjusts edge weights based on attribute similarity using the

Gaussian kernel, followed by local diffusion through a flow-based approach. [72] extracts noisy node labels from additional graph resources for diffusion on reweighted graphs. Unlike these methods requiring costly preprocessing as reported in Section VI, ours seamlessly integrate node attribute-derived affinities into the diffusion process, speeding up preprocessing and improving attribute utilization.

B. Community Search

Community search aims to search densely connected communities for a user-specified query [73], [74]. Similar to local clustering, community search is query-dependent and does not need to compute the graph globally. Researchers have devised different community models to define densely connected communities, including the most popular ones: k -core [75]–[77] and k -truss [78]–[80]. To incorporate attribute cohesiveness apart from structure cohesiveness, in recent years, a series of works [66], [80]–[83] on community search over attributed graphs have been developed. These methods usually consider keywords as the attributes of the nodes. Among these, ACQ [66], [81] and ATC [82] apply a core-based and a truss-based approach, respectively, both of which aimed at maximizing the number of keywords matching the query in the resulting community. Our approach differs as we do not use the intersections of keywords as the metric of attribute similarity. Although VAC [80] relaxes restrictions on using keywords as attributes, it still diverges from ours in both the objective and the method for calculating attribute similarity, especially in its repetitive computation to derive the minimum attribute similarity in the best k -truss. Another key difference is that community search literature imposes rigid topological constraints on the resulting community, which can lead to inferior outcomes. Moreover, these methods usually require offline index construction to enhance query processing speed, resulting in significant time and space overheads [32]. In contrast, our approach follows the LGC methods and designs an efficient attribute similarity computation method, eliminating the need for indices. Therefore, the problem setting of our work is orthogonal to that of community search.

VIII. CONCLUSION

In this paper, we present LACA, an effective approach that leverages node attributes to improve the LGC quality on attributed graphs. LACA achieves remarkable performance through four major contributions: (i) a novel problem formulation based on the novel node affinity measure BDD, (ii) an adaptive RWR-based graph diffusion algorithm with faster convergence, (iii) a highly scalable preprocessing technique that enables problem reduction, and (iv) a well-thought-out three-step scheme for BDD approximation. The superiority of LACA over 17 baselines is experimentally validated over 8 real datasets in terms of both clustering quality and practical efficiency. Regarding future work, we plan to study the local clustering on heterophilic graphs.

REFERENCES

- [1] C. Karras, A. Karras, I. Giannoukou, K. C. Giotopoulos, D. Tsolis, and S. Sioutas, "Global graph clustering and local graph exploration for community detection in twitter," in *2022 7th South-East Europe Design Automation, Computer Engineering, Computer Networks and Social Media Conference (SEEDA-CECNSM)*. IEEE, 2022, pp. 1–8.
- [2] X. Zhang, S. Xu, W. Lin, and S. Wang, "Constrained social community recommendation," in *Proceedings of the 29th ACM SIGKDD conference on knowledge discovery and data mining*, 2023, pp. 5586–5596.
- [3] J. Chen, O. Zaïane, and R. Goebel, "Local community identification in social networks," in *2009 international conference on advances in social network analysis and mining*. IEEE, 2009, pp. 237–242.
- [4] K. Voevodski, S.-H. Teng, and Y. Xia, "Finding local communities in protein networks," *BMC bioinformatics*, vol. 10, pp. 1–14, 2009.
- [5] C.-S. Liao, K. Lu, M. Baym, R. Singh, and B. Berger, "Isorankn: spectral methods for global alignment of multiple protein networks," *Bioinformatics*, vol. 25, pp. i253–i258, 2009.
- [6] J. Li, J. He, and Y. Zhu, "E-tail product return prediction via hypergraph-based local graph cut," in *Proceedings of the 24th ACM SIGKDD International Conference on Knowledge Discovery & Data Mining*, 2018, pp. 519–527.
- [7] Y. Zhu, J. Li, J. He, B. L. Quanz, and A. A. Deshpande, "A local algorithm for product return prediction in e-commerce," in *IJCAI*, 2018, pp. 3718–3724.
- [8] H. Yang, Y. Zhu, and J. He, "Local algorithm for user action prediction towards display ads," in *Proceedings of the 23rd ACM SIGKDD International Conference on Knowledge Discovery and Data Mining*, 2017, pp. 2091–2099.
- [9] A. Fazzzone, T. Lanciano, R. Denni, C. E. Tsourakakis, and F. Bonchi, "Discovering polarization niches via dense subgraphs with attractors and repulsers," *Proceedings of the VLDB Endowment*, vol. 15, no. 13, pp. 3883–3896, 2022.
- [10] D. F. Gleich and M. W. Mahoney, "Using local spectral methods to robustify graph-based learning algorithms," in *Proceedings of the 21th ACM SIGKDD International Conference on Knowledge Discovery and Data Mining*, 2015, pp. 359–368.
- [11] R. Rabbany, D. Bayani, and A. Dubrawski, "Active search of connections for case building and combating human trafficking," in *Proceedings of the 24th ACM SIGKDD International Conference on Knowledge Discovery & Data Mining*, 2018, pp. 2120–2129.
- [12] S. Maji, N. K. Vishnoi, and J. Malik, "Biased normalized cuts." IEEE, 2011.
- [13] M. W. Mahoney, L. Orecchia, and N. K. Vishnoi, "A local spectral method for graphs: With applications to improving graph partitions and exploring data graphs locally," *Journal of Machine Learning Research*, vol. 13, no. 77, pp. 2339–2365, 2012.
- [14] D. A. Spielman and S.-H. Teng, "A local clustering algorithm for massive graphs and its application to nearly linear time graph partitioning," *SIAM Journal on computing*, vol. 42, no. 1, pp. 1–26, 2013.
- [15] R. Andersen, F. Chung, and K. Lang, "Local graph partitioning using pagerank vectors," in *2006 47th Annual IEEE Symposium on Foundations of Computer Science (FOCS'06)*. IEEE, 2006, pp. 475–486.
- [16] K. Kloster and D. F. Gleich, "Heat kernel based community detection," in *Proceedings of the 20th ACM SIGKDD international conference on Knowledge discovery and data mining*, 2014, pp. 1386–1395.
- [17] R. Yang, X. Xiao, Z. Wei, S. S. Bhowmick, J. Zhao, and R.-H. Li, "Efficient estimation of heat kernel pagerank for local clustering," in *Proceedings of the 2019 International Conference on Management of Data*, 2019, pp. 1339–1356.
- [18] N. Masuda, M. A. Porter, and R. Lambiotte, "Random walks and diffusion on networks," *Physics reports*, vol. 716, pp. 1–58, 2017.
- [19] L. G. S. Jeub, P. Balachandran, M. A. Porter, P. J. Mucha, and M. W. Mahoney, "Think locally, act locally: Detection of small, medium-sized, and large communities in large networks," *Physical Review E*, vol. 91, 2015.
- [20] D. Wang, K. Fountoulakis, M. Henzinger, M. W. Mahoney, and S. Rao, "Capacity releasing diffusion for speed and locality," in *International Conference on Machine Learning*. PMLR, 2017, pp. 3598–3607.
- [21] K. Fountoulakis, D. Wang, and S. Yang, "p-norm flow diffusion for local graph clustering," in *International Conference on Machine Learning*. PMLR, 2020, pp. 3222–3232.
- [22] A. Jung and Y. SarcheshmehPour, "Local graph clustering with network lasso," *IEEE Signal Processing Letters*, vol. 28, pp. 106–110, 2020.
- [23] L. Lovász, "Random walks on graphs," *Combinatorics, Paul erdos is eighty*, vol. 2, no. 1–46, p. 4, 1993.
- [24] H. Yin, A. R. Benson, J. Leskovec, and D. F. Gleich, "Local higher-order graph clustering," in *Proceedings of the 23rd ACM SIGKDD international conference on knowledge discovery and data mining*, 2017, pp. 555–564.
- [25] D. Fu, D. Zhou, and J. He, "Local motif clustering on time-evolving graphs," in *Proceedings of the 26th ACM SIGKDD International conference on knowledge discovery & data mining*, 2020, pp. 390–400.
- [26] A. Chhabra, M. F. Faraj, and C. Schulz, "Local motif clustering via (hyper) graph partitioning," in *2023 Proceedings of the Symposium on Algorithm Engineering and Experiments (ALENEX)*. SIAM, 2023, pp. 96–109.
- [27] Z. Yuan, Z. Wei, F. Lv, and J.-R. Wen, "Index-free triangle-based graph local clustering," *Frontiers of Computer Science*, vol. 18, no. 3, p. 183404, 2024.
- [28] C. Huang, H. Li, Y. Zhang, W. Lei, and J. Lv, "Cross-space adaptive filter: Integrating graph topology and node attributes for alleviating the over-smoothing problem," in *Proceedings of the ACM on Web Conference 2024*, 2024, pp. 803–814.
- [29] L. Liao, X. He, H. Zhang, and T.-S. Chua, "Attributed social network embedding," *IEEE Transactions on Knowledge and Data Engineering*, vol. 30, no. 12, pp. 2257–2270, 2018.
- [30] C. Bothorel, J. D. Cruz, M. Magnani, and B. Mícenkova, "Clustering attributed graphs: models, measures and methods," *Network Science*, vol. 3, no. 3, pp. 408–444, 2015.
- [31] S. Freitas, N. Cao, Y. Xia, D. H. P. Chau, and H. Tong, "Local partition in rich graphs," in *2018 IEEE International Conference on Big Data (Big Data)*. IEEE, 2018, pp. 1001–1008.
- [32] Y. Niu, Y. Li, J. Fan, and Z. Bao, "Local clustering over labeled graphs: An index-free approach," in *2022 IEEE 38th International Conference on Data Engineering (ICDE)*. IEEE, 2022, pp. 2805–2817.
- [33] S. Yang and K. Fountoulakis, "Weighted flow diffusion for local graph clustering with node attributes: an algorithm and statistical guarantees," in *Proceedings of the 40th International Conference on Machine Learning*, vol. 202, 2023, pp. 39252–39276.
- [34] N. Halko, P.-G. Martinsson, and J. A. Tropp, "Finding structure with randomness: Probabilistic algorithms for constructing approximate matrix decompositions," *SIAM review*, vol. 53, no. 2, pp. 217–288, 2011.
- [35] F. X. X. Yu, A. T. Suresh, K. M. Choromanski, D. N. Holtmann-Rice, and S. Kumar, "Orthogonal random features," *Advances in neural information processing systems*, vol. 29, 2016.
- [36] S. Wang, R. Yang, X. Xiao, Z. Wei, and Y. Yang, "Fora: simple and effective approximate single-source personalized pagerank," in *Proceedings of the ACM SIGKDD International Conference on Knowledge Discovery and Data Mining*, 2017, pp. 505–514.
- [37] R. Yang, "Efficient and effective similarity search over bipartite graphs," in *Proceedings of the ACM Web Conference 2022*, 2022, pp. 308–318.
- [38] W. L. Hamilton, Z. Ying, and J. Leskovec, "Inductive representation learning on large graphs," vol. 30, 2017, pp. 1024–1034.
- [39] B. Li, B. Jing, and H. Tong, "Graph communal contrastive learning," *Proceedings of the ACM Web Conference 2022*, 2022.
- [40] H. Tong, C. Faloutsos, and J.-Y. Pan, "Fast random walk with restart and its applications," in *Sixth international conference on data mining (ICDM'06)*. IEEE, 2006, pp. 613–622.
- [41] G. Jeh and J. Widom, "Scaling personalized web search," in *Proceedings of the 12th international conference on World Wide Web*, 2003, pp. 271–279.
- [42] S. Rothe and H. Schütze, "Cosimrank: A flexible & efficient graph-theoretic similarity measure," in *Proceedings of the 52nd Annual Meeting of the Association for Computational Linguistics*, 2014, pp. 1392–1402.
- [43] P. Lofgren, S. Banerjee, and A. Goel, "Bidirectional pagerank estimation: From average-case to worst-case," in *Algorithms and Models for the Web Graph: 12th International Workshop, WAW 2015, Eindhoven, The Netherlands, December 10-11, 2015, Proceedings 12*. Springer, 2015, pp. 164–176.
- [44] R. J. Muirhead, *Aspects of multivariate statistical theory*. John Wiley & Sons, 2009.
- [45] Y. Ma, X. Liu, T. Zhao, Y. Liu, J. Tang, and N. Shah, "A unified view on graph neural networks as graph signal denoising," in *Proceedings of the 30th ACM International Conference on Information & Knowledge Management*, 2021, pp. 1202–1211.

- [46] M. Zhu, X. Wang, C. Shi, H. Ji, and P. Cui, "Interpreting and unifying graph neural networks with an optimization framework," in *Proceedings of the Web Conference 2021*, 2021, pp. 1215–1226.
- [47] A. Bojchevski, J. Gasteiger, B. Perozzi, A. Kapoor, M. Blais, B. Rózemberczki, M. Lukasik, and S. Günnemann, "Scaling graph neural networks with approximate pagerank," in *Proceedings of the 26th ACM SIGKDD International Conference on Knowledge Discovery & Data Mining*, 2020, pp. 2464–2473.
- [48] P. Sen, G. Namata, M. Bilgic, L. Getoor, B. Galligher, and T. Eliassirad, "Collective classification in network data," *AI magazine*, vol. 29, no. 3, pp. 93–93, 2008.
- [49] L. Tang and H. Liu, "Relational learning via latent social dimensions," in *Proceedings of the 15th ACM SIGKDD international conference on Knowledge discovery and data mining*, 2009, pp. 817–826.
- [50] X. Huang, J. Li, and X. Hu, "Label informed attributed network embedding," in *Proceedings of the tenth ACM international conference on web search and data mining*, 2017, pp. 731–739.
- [51] W. Hu, M. Fey, M. Zitnik, Y. Dong, H. Ren, B. Liu, M. Catasta, and J. Leskovec, "Open graph benchmark: Datasets for machine learning on graphs," *Advances in neural information processing systems*, vol. 33, pp. 22 118–22 133, 2020.
- [52] H. Zeng, H. Zhou, A. Srivastava, R. Kannan, and V. K. Prasanna, "Graphsaint: Graph sampling based inductive learning method," in *The 8th International Conference on Learning Representations*, 2023.
- [53] W.-L. Chiang, X. Liu, S. Si, Y. Li, S. Bengio, and C.-J. Hsieh, "Cluster-gcn: An efficient algorithm for training deep and large graph convolutional networks," in *Proceedings of the 25th ACM SIGKDD international conference on knowledge discovery & data mining*, 2019, pp. 257–266.
- [54] D. Liben-Nowell and J. Kleinberg, "The link prediction problem for social networks," in *Proceedings of the twelfth international conference on Information and knowledge management*, 2003, pp. 556–559.
- [55] G. Jeh and J. Widom, "Simrank: a measure of structural-context similarity," in *Proceedings of the eighth ACM SIGKDD international conference on Knowledge discovery and data mining*, 2002, pp. 538–543.
- [56] Z. Yin, M. Gupta, T. Weninger, and J. Han, "A unified framework for link recommendation using random walks." IEEE, 2010.
- [57] F. Rahutomo, T. Kitasuka, and M. Aritsugi, "Semantic cosine similarity," in *The 7th international student conference on advanced science and technology ICAST*, vol. 4, no. 1, 2012, p. 1.
- [58] C.-C. Hsu, Y.-A. Lai, W.-H. Chen, M.-H. Feng, and S.-D. Lin, "Unsupervised ranking using graph structures and node attributes." ACM, 2017.
- [59] A. Grover and J. Leskovec, "node2vec: Scalable feature learning for networks," *Proceedings of the 22nd ACM SIGKDD International Conference on Knowledge Discovery and Data Mining*, 2016.
- [60] R. Yang, J. Shi, X. Xiao, Y. Yang, J. Liu, S. S. Bhowmick et al., "Scaling attributed network embedding to massive graphs," *Proceedings of the VLDB Endowment*, vol. 14, no. 1, pp. 37–49, 2020.
- [61] R. Yang, J. Shi, X. Xiao, Y. Yang, S. S. Bhowmick, and J. Liu, "Pane: scalable and effective attributed network embedding," *The VLDB Journal*, vol. 32, pp. 1237–1262, 2023.
- [62] G. Pan, Y. Yao, H. Tong, F. Xu, and J. Lu, "Unsupervised attributed network embedding via cross fusion." ACM, 2021.
- [63] K. Fountoulakis, D. F. Gleich, and M. W. Mahoney, "A short introduction to local graph clustering methods and software," 2018.
- [64] A. Hagberg, P. Swart, and D. S. Chult, "Exploring network structure, dynamics, and function using networkx," Los Alamos National Lab.(LANL), Los Alamos, NM (United States), Tech. Rep., 2008.
- [65] F. Chung, "The heat kernel as the pagerank of a graph," *Proceedings of the National Academy of Sciences*, vol. 104, no. 50, pp. 19 735–19 740, 2007.
- [66] Y. Fang, R. Cheng, S. Luo, and J. Hu, "Effective community search for large attributed graphs," vol. 9. Association for Computing Machinery (ACM), 2016, pp. 1233–1244.
- [67] Y. Fang, Z. Wang, R. Cheng, H. Wang, and J. Hu, "Effective and efficient community search over large directed graphs," *IEEE Transactions on Knowledge and Data Engineering*, vol. 31, no. 11, pp. 2093–2107, 2018.
- [68] Y. Fang, Y. Yang, W. Zhang, X. Lin, and X. Cao, "Effective and efficient community search over large heterogeneous information networks," vol. 13, no. 6. VLDB Endowment, 2020, pp. 854–867.
- [69] J. Zhang, J. Tang, C. Ma, H. Tong, Y. Jing, and J. Li, "Panther: Fast top-k similarity search on large networks," in *Proceedings of the 21th ACM SIGKDD international conference on knowledge discovery and data mining*, 2015, pp. 1445–1454.
- [70] G. Baltasou, K. Christopoulos, and K. Tsihlias, "Local community detection: A survey," *IEEE Access*, vol. 10, pp. 110 701–110 726, 2022.
- [71] R. Andersen, S. O. Gharan, Y. Peres, and L. Trevisan, "Almost optimal local graph clustering using evolving sets," *Journal of the ACM (JACM)*, vol. 63, no. 2, pp. 1–31, 2016.
- [72] A. B. de Luca, K. Fountoulakis, and S. Yang, "Local graph clustering with noisy labels," in *The Twelfth International Conference on Learning Representations*, 2023.
- [73] X. Huang, L. V. Lakshmanan, and J. Xu, *Community Search over Big Graphs*. Morgan & Claypool Publishers, 2019.
- [74] —, "Community search over big graphs: Models, algorithms, and opportunities," in *Proceedings of the 33rd IEEE International Conference on Data Engineering (ICDE)*, 2017, pp. 1451–1454.
- [75] M. Sozio and A. Gionis, "The community-search problem and how to plan a successful cocktail party." ACM, 2010.
- [76] W. Cui, Y. Xiao, H. Wang, and W. Wang, "Local search of communities in large graphs." ACM, 2014.
- [77] N. Barbieri, F. Bonchi, E. Galimberti, and F. Gullo, "Efficient and effective community search," *Data Mining and Knowledge Discovery*, vol. 29, pp. 1406–1433, 2015.
- [78] X. Huang, H. Cheng, L. Qin, W. Tian, and J. X. Yu, "Querying k-truss community in large and dynamic graphs." ACM, 2014.
- [79] X. Huang, L. V. S. Lakshmanan, J. X. Yu, and H. Cheng, "Approximate closest community search in networks," vol. 9. Association for Computing Machinery (ACM), 2015, pp. 276–287.
- [80] Q. Liu, Y. Zhu, M. Zhao, X. Huang, J. Xu, and Y. Gao, "Vac: Vertex-centric attributed community search." IEEE, 2020.
- [81] Y. Fang, R. Cheng, Y. Chen, S. Luo, and J. Hu, "Effective and efficient attributed community search," *The VLDB Journal*, vol. 26, pp. 803–828, 2017.
- [82] X. Huang and L. V. S. Lakshmanan, "Attribute-driven community search," vol. 10. Association for Computing Machinery (ACM), 2017, pp. 949–960.
- [83] Y. Zhu, J. He, J. Ye, L. Qin, X. Huang, and J. X. Yu, "When structure meets keywords: Cohesive attributed community search." ACM, 2020.
- [84] G. H. Golub and C. F. Van Loan, "Matrix computations," *Johns Hopkins University Press, 3rd edition*, 1996.
- [85] G. Strang, *Introduction to linear algebra*. SIAM, 2022.
- [86] Z. Zhang, P. Cui, X. Wang, J. Pei, X. Yao, and W. Zhu, "Arbitrary-order proximity preserved network embedding," in *Proceedings of the 24th ACM SIGKDD international conference on knowledge discovery & data mining*, 2018, pp. 2778–2786.
- [87] J. MacQueen et al., "Some methods for classification and analysis of multivariate observations," in *Proceedings of the fifth Berkeley symposium on mathematical statistics and probability*, vol. 1, no. 14. Oakland, CA, USA, 1967, pp. 281–297.
- [88] J. Yang and J. Leskovec, "Defining and evaluating network communities based on ground-truth." IEEE, 2012.
- [89] C. Yang, Z. Liu, D. Zhao, M. Sun, and E. Y. Chang, "Network representation learning with rich text information," in *Proceedings of the Thirty-Second International Joint Conference on Artificial Intelligence*. International Joint Conferences on Artificial Intelligence Organization, 2015, pp. 2111–2117.
- [90] X. Huang, J. Li, and X. Hu, "Accelerated attributed network embedding," vol. Not available. Society for Industrial and Applied Mathematics, 2017, pp. 633–641.
- [91] H. Yang, S. Pan, L. Chen, C. Zhou, and P. Zhang, "Low-bit quantization for attributed network representation learning." International Joint Conferences on Artificial Intelligence Organization, 2019.
- [92] Z. Zhang, H. Yang, J. Bu, S. Zhou, P. Yu, J. Zhang, M. Ester, and C. Wang, "Anrl: Attributed network representation learning via deep neural networks." International Joint Conferences on Artificial Intelligence Organization, 2018.
- [93] H. Gao and H. Huang, "Deep attributed network embedding." International Joint Conferences on Artificial Intelligence Organization, 2018.
- [94] T. Mikolov, I. Sutskever, K. Chen, G. S. Corrado, and J. Dean, "Distributed representations of words and phrases and their compositionality," vol. 26, 2013, pp. 3111–3119.

A. Theoretical Proofs

1) Proof of Theorem IV.1:

Proof. We denote $\vec{\gamma}^\ell$ as the vector $\vec{\gamma}$ obtained at Line 3 and by \vec{b}^ℓ the remaining residual at Line 5 in ℓ -th iteration. Then, according to Line 6, \vec{q} can be represented by

$$\vec{q} = (1 - \alpha) \sum_{\ell} \vec{\gamma}^\ell. \quad (21)$$

Next, we consider $\{\vec{\gamma}^1, \vec{\gamma}^2, \dots, \vec{\gamma}^\ell, \vec{\gamma}^{\ell+1}, \dots, \vec{\gamma}^\infty\}$. By Lines 3 and 7-8, we have

$$\begin{aligned} \vec{\gamma}^1 &= \vec{f} - \vec{b}^1, \quad \vec{\gamma}^1 = \vec{b}^1 + \alpha \vec{\gamma}^1 \mathbf{P} - \vec{b}^2 \\ \dots \\ \vec{\gamma}^\ell &= \vec{b}^{\ell-1} + \alpha \vec{\gamma}^{\ell-1} \mathbf{P} - \vec{b}^\ell, \quad \vec{\gamma}^{\ell+1} = \vec{b}^\ell + \alpha \vec{\gamma}^\ell \mathbf{P} - \vec{b}^{\ell+1} \\ \dots \end{aligned}$$

Then, Eq. (21) can be rewritten as

$$\begin{aligned} \frac{\vec{q}}{1 - \alpha} &= \vec{f} + \alpha \sum_{\ell=1}^{\infty} \vec{\gamma}^\ell \mathbf{P} - \vec{b}^\infty \\ &= \sum_{\ell=0}^{\infty} \alpha^\ell \vec{f} \mathbf{P}^\ell - \sum_{\ell=0}^{\infty} \alpha^\ell \vec{b}^\ell \mathbf{P}^\ell. \end{aligned} \quad (22)$$

Recall that \vec{b}^ℓ always satisfies $\forall v_i \in \mathcal{V}$, $\vec{b}_i^\ell / d(v_i) < \epsilon$ (see Lines 3 and 5). Let \vec{b} be a length- n vector where each i -th entry is $\epsilon \cdot d(v_i)$. Together with Eq. (22) and the matrix definition of $\pi(v_i, v_j)$ defined in Eq. (6), we can bound each entry \vec{q}_t by

$$\begin{aligned} \vec{q}_t &\geq (1 - \alpha) \sum_{\ell=0}^{\infty} \alpha^\ell (\vec{f} \mathbf{P}^\ell)_t - (1 - \alpha) \sum_{\ell=0}^{\infty} \alpha^\ell (\vec{b} \mathbf{P}^\ell)_t \\ &= \sum_{v_i \in \mathcal{V}} \vec{f}_i \cdot \pi(v_i, v_t) - \sum_{v_i \in \mathcal{V}} \vec{b}_i \cdot \pi(v_i, v_t) \\ &= \sum_{v_i \in \mathcal{V}} \vec{f}_i \cdot \pi(v_i, v_t) - \sum_{v_i \in \mathcal{V}} \epsilon \cdot d(v_i) \cdot \pi(v_i, v_t). \end{aligned}$$

By the fact of $d(v_i) \cdot \pi(v_i, v_t) = d(v_t) \cdot \pi(v_t, v_i)$ (Lemma 1 in [43]) and $\sum_{v_i \in \mathcal{V}} \pi(v_t, v_i) = 1$, the above inequality can be simplified as

$$\begin{aligned} \vec{q}_t &\geq \sum_{v_i \in \mathcal{V}} \vec{f}_i \cdot \pi(v_i, v_t) - \epsilon \cdot d(v_t) \cdot \sum_{v_i \in \mathcal{V}} \pi(v_t, v_i) \\ &= \sum_{v_i \in \mathcal{V}} \vec{f}_i \cdot \pi(v_i, v_t) - \epsilon \cdot d(v_t), \end{aligned}$$

which finishes the proof of Eq. (14).

In what follows, we analyze the time complexity of Algo. (1). First, suppose that Lines 3-7 in Algo. 1 are executed for L iterations. Now, we consider any iteration ℓ . For ease of exposition, we denote $\vec{\gamma}^\ell$ as the vector $\vec{\gamma}$ obtained at Line 3 in ℓ -th iteration and by \vec{r}^ℓ and \vec{q}^ℓ the residual and reserve vectors \vec{r} and \vec{q} at the beginning of ℓ -th iteration, respectively. Accordingly, for each non-zero entry $\vec{\gamma}_i^\ell$ in $\vec{\gamma}^\ell$, $\vec{\gamma}_i^\ell \geq d(v_i) \cdot \epsilon$.

First, we prove that at the beginning of any ℓ -th iteration, the following equation holds:

$$\|\vec{r}^\ell\|_1 + \|\vec{q}^\ell\|_1 = \|\vec{f}\|_1. \quad (23)$$

We prove this by induction. For the base case where $\ell = 1$, i.e., at the beginning of the first iteration, we have $\vec{r}^1 = \vec{f}$ and $\vec{q}^1 = \mathbf{0}$, and thus, Eq. (23) holds. Next, we assume Eq. (23) holds at the beginning of ℓ -th ($\ell > 0$) iteration, i.e., $\|\vec{r}^\ell\|_1 + \|\vec{q}^\ell\|_1 = \|\vec{f}\|_1$. According to Lines 5-7, we have

$$\begin{aligned} \vec{q}^{\ell+1} &= \vec{q}^\ell + (1 - \alpha) \cdot \vec{\gamma}^\ell \\ \vec{r}^{\ell+1} &= \vec{r}^\ell - \vec{\gamma}^\ell + \alpha \cdot \vec{\gamma}^\ell \mathbf{P}. \end{aligned}$$

As such,

$$\begin{aligned} \|\vec{r}^{\ell+1}\|_1 + \|\vec{q}^{\ell+1}\|_1 &= \|\vec{q}^\ell\|_1 + \|\vec{r}^\ell\|_1 + \alpha \cdot \|\vec{\gamma}^\ell \mathbf{P} - \vec{\gamma}^\ell\|_1. \end{aligned} \quad (24)$$

Note that

$$\begin{aligned} \|\vec{\gamma}^\ell \mathbf{P} - \vec{\gamma}^\ell\|_1 &= \sum_{v_i \in \mathcal{V}} \sum_{v_j \in \mathcal{V}} \vec{\gamma}_j^\ell \cdot \mathbf{P}_{j,i} - \sum_{v_j \in \mathcal{V}} \vec{\gamma}_j^\ell \\ &= \sum_{v_j \in \mathcal{V}} \vec{\gamma}_j^\ell \sum_{v_i \in \mathcal{V}} \mathbf{P}_{j,i} - \sum_{v_j \in \mathcal{V}} \vec{\gamma}_j^\ell \\ &= \sum_{v_j \in \mathcal{V}} \vec{\gamma}_j^\ell \sum_{v_i \in \mathcal{N}(v_j)} \frac{1}{d(v_j)} - \sum_{v_j \in \mathcal{V}} \vec{\gamma}_j^\ell = 0, \end{aligned}$$

implying that $\|\vec{r}^{\ell+1}\|_1 + \|\vec{q}^{\ell+1}\|_1$ in Eq. (24) equals 0, namely, Eq. (23) still holds.

As per Line 6, in each ℓ -th iteration, Algo. 1 converts $(1 - \alpha)$ fraction of $\vec{\gamma}^\ell$ into \vec{q}^ℓ , i.e., at least $(1 - \alpha) \cdot \epsilon \cdot d(v_i)$ out of each non-zero entries in $\vec{\gamma}^\ell$ is passed to \vec{q}^ℓ . After L iterations, we obtain \vec{q}^L . Recall that by Eq. (23), $\|\vec{q}^L\|_1 \leq \|\vec{f}\|_1$. We obtain

$$\sum_{\ell=1}^L \sum_{i \in \text{supp}(\vec{\gamma}^\ell)} (1 - \alpha) \cdot \epsilon \cdot d(v_i) \leq \|\vec{q}^L\|_1 \leq \|\vec{f}\|_1, \quad (25)$$

which leads to $\sum_{\ell=1}^L \sum_{i \in \text{supp}(\vec{\gamma}^\ell)} d(v_i) \leq \frac{\|\vec{f}\|_1}{(1 - \alpha)\epsilon}$.

Notice that in Line 6, each non-zero entry in $\vec{\gamma}^\ell$ will result in $d(v_i)$ operations in the matrix-vector multiplication $\vec{\gamma}^\ell \mathbf{P}$. Thus, the total cost of Line 6 for L iterations is $\sum_{\ell=1}^L \sum_{i \in \text{supp}(\vec{\gamma}^\ell)} d(v_i)$, which is bounded by $\frac{\|\vec{f}\|_1}{(1 - \alpha)\epsilon}$ as aforementioned. In addition, in each iteration, Lines 5 and 7 also merely involve operations on the non-zero entries in $\vec{\gamma}^\ell$. Their total cost for L iterations can then be bounded by $\frac{\|\vec{f}\|_1}{(1 - \alpha)\epsilon}$ as well. As for Line 3, in the first iteration, we need to inspect every entry in \vec{r}^1 , and hence, the time cost is $\|\vec{r}^1\|_0 = |\text{supp}(\vec{f})|$. In any subsequent ℓ -th iteration, we solely need to inspect the entries in \vec{r}^ℓ affected by Line 7 in the previous iteration, which is also bounded by the non-zero entries in $\vec{\gamma}^{\ell-1}$. Hence, the overall time complexity of Algo. 1 is $O\left(\max\left\{|\text{supp}(\vec{f})|, \frac{\|\vec{f}\|_1}{(1 - \alpha)\epsilon}\right\}\right)$. The theorem is proved. \square

2) Proof of Theorem IV.2:

Proof. Similar to the proof of Theorem IV.1, we let \vec{b}^ℓ be the remaining residual in the ℓ -th iteration in Algo. 2. By Lines 6 and Lines 8-11, Eq. (22) still holds. Notice that \vec{b}^ℓ is 0 when ℓ -th iteration runs Lines 5-6. As such, \vec{b}^ℓ always satisfies $\forall v_i \in \mathcal{V}, \frac{\vec{b}_i^\ell}{d(v_i)} < \epsilon$ and then Eq. (14) follows as in the proof of Theorem IV.1.

Next, we analyze the time complexity of Algo. 2. Notice that according to Line 4 in Algo. (2), the total cost C_{tot} entailed by the non-greedy operations (Lines 4-6) is bounded by $O\left(\frac{\|\vec{f}\|_1}{(1-\alpha)\epsilon}\right)$. As for greedy operations (Lines 8-11), they will be conducted as in Algo. (1). Note that Algo. 2 also terminates when \vec{r} is 0. Therefore, the total amount of greedy operations in AdaptiveDiffuse is at most that needed in GreedyDiffuse (see Theorem IV.1). In sum, the overall complexity of Algo. 2 is $O\left(\max\left\{\left|\text{supp}(\vec{f})\right|, \frac{\|\vec{f}\|_1}{(1-\alpha)\epsilon}\right\}\right)$. \square

3) Proof of Lemma IV.3:

Proof. We assume Algo. 2 conducts Lines 3-11 for L iterations, and we refer to the vectors \vec{q} , \vec{r} , and \vec{r}^j in each ℓ -th iteration as in the proof of Theorem IV.1. Further, we assume that in ℓ_1 -th, ℓ_2 -th, ..., and ℓ_T -th iterations, AdaptiveDiffuse executes Lines 8-11. Based on Inequality (25) and Eq. (23), we can get

$$\sum_{j=1}^T \sum_{i \in \text{supp}(\vec{r}^{\ell_j})} d(v_i) \leq \frac{\|\vec{q}^{\ell_T}\|_1}{(1-\alpha)\epsilon} \leq \frac{\|\vec{f}\|_1 - \|\vec{r}^{\ell_T}\|_1}{(1-\alpha)\epsilon}.$$

Let $\mathcal{L} = \{1, 2, \dots, L\}$ and $\mathcal{T} = \{\ell_1, \ell_2, \dots, \ell_T\}$. As for the $\mathcal{L} \setminus \mathcal{T}$ iterations, Algo. (2) conducts Lines 5-6. Notice that in such cases, we have $C_{tot} + \text{vol}(\vec{r}) < \frac{\|\vec{f}\|_1}{(1-\alpha)\epsilon}$, meaning that

$$\sum_{j \in \mathcal{L} \setminus \mathcal{T}} \sum_{i \in \text{supp}(\vec{r}^j)} d(v_i) \leq \frac{\|\vec{f}\|_1}{(1-\alpha)\epsilon}.$$

According to Lines 5-6 and Lines 8-11, all the non-zero elements in final \vec{q} are from non-zero entries in $\vec{r}^j \forall j \in \mathcal{T}$ and $\vec{r}^j \forall j \in \mathcal{L} \setminus \mathcal{T}$. Then,

$$\begin{aligned} \text{vol}(\vec{q}) &= \sum_{i \in \text{supp}(\vec{q})} d(v_i) \\ &\leq \sum_{j=1}^T \sum_{i \in \text{supp}(\vec{r}^{\ell_j})} d(v_i) + \sum_{j \in \mathcal{L} \setminus \mathcal{T}} \sum_{i \in \text{supp}(\vec{r}^j)} d(v_i) \\ &\leq \frac{2\|\vec{f}\|_1 - \|\vec{r}^{\ell_T}\|_1}{(1-\alpha)\epsilon} = \frac{\beta\|\vec{f}\|_1}{(1-\alpha)\epsilon}, \end{aligned}$$

where β stands for a constant in the range $[1, 2]$ since $0 \leq \|\vec{r}^{\ell_T}\|_1 \leq \|\vec{f}\|_1$. Similarly, we obtain

$$|\text{supp}(\vec{q})| \leq \sum_{i \in \text{supp}(\vec{q})} d(v_i) = \text{vol}(\vec{q}) \leq \frac{\beta\|\vec{f}\|_1}{(1-\alpha)\epsilon}.$$

When $\sigma \geq 1$, AdaptiveDiffuse only executes Lines 8-11, and thus, $\mathcal{L} \setminus \mathcal{T}$ is an empty set. The above inequalities become

$$|\text{supp}(\vec{q})| \leq \text{vol}(\vec{q}) \leq \frac{\|\vec{f}\|_1}{(1-\alpha)\epsilon},$$

which completes the proof. \square

4) Proof of Lemma V.1:

Proof. We first need the following theorem.

Theorem A.1 (Eckart–Young Theorem [84]). *Suppose that $M_k \in \mathbb{R}^{n \times k}$ is the rank- k approximation to $M \in \mathbb{R}^{n \times n}$ obtained by exact SVD, then $\min_{\text{rank}(\widehat{M}) \leq k} \|M - \widehat{M}\|_2 = \|M - M_k\|_2 = \lambda_{k+1}$, where λ_{k+1} stands for the $(k+1)$ -th largest singular value of M .*

Suppose that $U\Lambda V^\top$ is the exact k -SVD of X , by Theorem A.1, we have $\|U\Lambda V^\top - X\|_2 \leq \lambda_{k+1}$, where λ_{k+1} is the $(k+1)$ -th largest singular value of X . Let $\widehat{U}\widehat{\Lambda}\widehat{V}^\top$ be the k -SVD of XX^\top . Similarly, from Theorem A.1, we get $\|\widehat{U}\widehat{\Lambda}\widehat{V}^\top - XX^\top\|_2 \leq \widehat{\lambda}_{k+1}$, where $\widehat{\lambda}_{k+1}$ is the $(k+1)$ -th largest singular value of XX^\top .

According to [85], columns in U are the eigenvectors of matrix XX^\top and the squared singular values of X are the eigenvalues of XX^\top . Given that singular values are non-negative, all the eigenvalues of XX^\top are also non-negative. Λ^2 and U contain the k -largest eigenvalues and corresponding eigenvectors of XX^\top , and $\lambda_{k+1}^2 = \widehat{\lambda}_{k+1}$. Further, by Theorem 4.1 in [86], it can be verified that Λ^2 and U are the top- k singular values and left/right singular vectors of XX^\top , respectively, and λ_{k+1}^2 is the $(k+1)$ -th largest singular value of XX^\top . Consequently, $\|U\Lambda^2U^\top - XX^\top\|_2 \leq \lambda_{k+1}^2$ and the proof is done. \square

5) Proof of Theorem V.2:

Proof. Recall that for $v_i \in \mathcal{V}$, vector $\vec{x}^{(i)}$ is L_2 normalized, i.e., $\|\vec{x}^{(i)}\|_2 = 1$. Thus, we can derive $\|\vec{x}^{(i)} - \vec{x}^{(j)}\|_2^2 = 2(1 - \cos(\vec{x}^{(i)}, \vec{x}^{(j)})) = 2(1 - \vec{x}^{(i)} \cdot \vec{x}^{(j)}) \in [0, 4]$. On its basis, $f(v_i, v_j)$ in Eq. (3) can be transformed as follows:

$$\begin{aligned} f(v_i, v_j) &= \exp\left(\frac{\vec{x}^{(i)} \cdot \vec{x}^{(j)}}{\delta}\right) = \exp\left(\frac{1 - \frac{1}{2}\|\vec{x}^{(i)} - \vec{x}^{(j)}\|_2^2}{\delta}\right) \\ &= \exp\left(\frac{1}{\delta} - \frac{\|\vec{x}^{(i)} - \vec{x}^{(j)}\|_2^2}{2\delta}\right) \\ &= \exp\left(\frac{1}{\delta}\right) \cdot \exp\left(-\frac{\|\vec{x}^{(i)} - \vec{x}^{(j)}\|_2^2}{2\delta}\right). \end{aligned} \quad (26)$$

According to Theorem 1 in [35] and the mathematical form of $\widehat{Y} = \frac{1}{\delta}X\Sigma Q = \frac{1}{\delta}U\Lambda\Sigma Q$ via Lines 6-9, we have

$$\mathbb{E}[\mathbf{K} \cdot \mathbf{K}^\top] = \exp\left(-\frac{\|\vec{x}^{(i)} - \vec{x}^{(j)}\|_2^2}{2\delta}\right),$$

where $\mathbf{K} = \frac{1}{\sqrt{d}} \cdot \sin(\vec{y}^{(i)}) \parallel \cos(\vec{y}^{(j)})$. Plugging the definitions of $f(v_i, v_j)$ in Eq. (26) and \mathbf{Y} in Eq. (19) into the above equation proves the theorem. \square

6) *Proof of Lemma V.3:*

Proof. According to [34], the invocation of k -SVD over \mathbf{X} runs in $O(ndk + nk^2)$ time. Note that the number of iterations in k -SVD is regarded as a constant and thus is omitted since it is set to small integers, e.g., 7, in practice, and k is less than d . By Eq. (18), the computations of $\vec{\mathbf{y}}^*$ and $\vec{\mathbf{z}}^{(i)} \forall v_i \in \mathcal{V}$ at Lines 10-11 need $O(nk)$ time. Thus, when $f(\cdot, \cdot)$ is the cosine similarity function, the construction of TNAM \mathbf{Z} requires $O(ndk)$ time.

In comparison, when $f(\cdot, \cdot)$ is the exponential cosine similarity function, the QR decomposition at Line 7 and constructing \mathbf{Y} at Line 9 take $O(k^3)$ and $O(nk^2)$ time, respectively. In turn, the overall time complexity of Algo. 3 is bounded by $O(ndk)$, which can be reduced to $O(nd)$ since k is regarded as a constant. \square

7) *Proof of Theorem V.4:*

Proof. Let $\vec{\rho}^\circ$ be the vector returned by Algo. 2 invoked at Line 5 in Algo. 4. According to Theorem IV.2, $\forall v_j \in \mathcal{V}$,

$$\sum_{j \in \text{supp}(\vec{\pi}')} \sum_{v_i \in \mathcal{V}} \vec{\pi}'_i \cdot s(v_i, v_j) \cdot d(v_j) \cdot \pi(v_j, v_t) - \vec{\rho}_t^\circ \geq 0 \text{ and}$$

$$\sum_{j \in \text{supp}(\vec{\pi}')} \sum_{v_i \in \mathcal{V}} \vec{\pi}'_i \cdot s(v_i, v_j) \cdot d(v_j) \cdot \pi(v_j, v_t) - \vec{\rho}_t^\circ \leq \epsilon \cdot d(v_t),$$

yielding

$$0 \leq \sum_{j \in \text{supp}(\vec{\pi}')} \sum_{v_i \in \mathcal{V}} \vec{\pi}'_i \cdot s(v_i, v_j) \cdot \frac{d(v_j)}{d(v_t)} \cdot \pi(v_j, v_t) - \frac{\vec{\rho}_t^\circ}{d(v_t)} \leq \epsilon.$$

By the fact of $\pi(v_t, v_j) = \frac{d(v_j)}{d(v_t)} \cdot \pi(v_j, v_t)$ (Lemma 1 in [43]) and $\vec{\rho}_t' = \frac{\vec{\rho}_t^\circ}{d(v_t)}$ (Line 6), we have

$$0 \leq \sum_{j \in \text{supp}(\vec{\pi}')} \sum_{v_i \in \mathcal{V}} \vec{\pi}'_i \cdot s(v_i, v_j) \cdot \pi(v_t, v_j) - \vec{\rho}_t' \leq \epsilon.$$

Further, we obtain

$$\vec{\rho}_t' \leq \sum_{j \in \text{supp}(\vec{\pi}')} \sum_{v_i \in \mathcal{V}} \vec{\pi}'_i \cdot s(v_i, v_j) \cdot \pi(v_t, v_j)$$

$$\vec{\rho}_t' \geq \sum_{j \in \text{supp}(\vec{\pi}')} \sum_{v_i \in \mathcal{V}} \vec{\pi}'_i \cdot s(v_i, v_j) \cdot \pi(v_t, v_j) - \epsilon.$$

Notice that $\vec{\pi}$ obtained at Line 2 in Algo. 4 satisfies $0 \leq \pi(v_s, v_i) - \vec{\pi}'_i \leq \epsilon \cdot d(v_i) \forall v_i \in \mathcal{V}$ according to Theorem IV.2. We then derive

$$\vec{\rho}_t' \leq \sum_{j \in \text{supp}(\vec{\pi}')} \sum_{v_i \in \mathcal{V}} \pi(v_s, v_i) \cdot s(v_i, v_j) \cdot \pi(v_t, v_j) \leq \vec{\rho}_t$$

and

$$\vec{\rho}_t' \geq \sum_{j \in \text{supp}(\vec{\pi}')} \sum_{v_i \in \mathcal{V}} (\pi(v_s, v_i) - \epsilon d(v_i)) \cdot s(v_i, v_j) \cdot \pi(v_t, v_j) - \epsilon,$$

where the latter leads to

$$\vec{\rho}_t - \vec{\rho}_t' \leq \epsilon + \sum_{j \in \text{supp}(\vec{\pi}')} \sum_{v_i \in \mathcal{V}} \epsilon d(v_i) \cdot s(v_i, v_j) \cdot \pi(v_t, v_j)$$

$$+ \sum_{j \in \{1, \dots, n\} \setminus \text{supp}(\vec{\pi}')} \sum_{v_i \in \mathcal{V}} \pi(v_s, v_i) \cdot s(v_i, v_j) \cdot \pi(v_t, v_j).$$

Recall that $0 \leq \pi(v_s, v_i) - \vec{\pi}'_i \leq \epsilon \cdot d(v_i) \forall v_i \in \mathcal{V}$. Thus, $\forall i \notin \text{supp}(\vec{\pi}')$, $\pi(v_s, v_i) \leq \vec{\pi}'_i + \epsilon \cdot d(v_i) = \epsilon \cdot d(v_i)$. Accordingly,

$$\vec{\rho}_t - \vec{\rho}_t' \leq \epsilon + \sum_{v_j \in \mathcal{V}} \sum_{v_i \in \mathcal{V}} \epsilon d(v_i) \cdot s(v_i, v_j) \cdot \pi(v_t, v_j)$$

$$\leq \epsilon + \sum_{v_i \in \mathcal{V}} \epsilon d(v_i) \cdot \sum_{v_j \in \mathcal{V}} s(v_i, v_j) \cdot \pi(v_t, v_j)$$

$$\leq (1 + \sum_{v_i \in \mathcal{V}} d(v_i) \cdot \max_{v_j \in \mathcal{V}} s(v_i, v_j)) \cdot \epsilon,$$

which proves the theorem. \square

8) *Proof of Lemma V.6:*

Proof. By setting its derivative w.r.t. \mathbf{H} to zero and , we obtain the optimal \mathbf{H} as:

$$\frac{\partial \{(1 - \alpha) \cdot \|\mathbf{H} - \mathbf{H}^\circ\|_F^2 + \alpha \cdot \text{trace}(\mathbf{H}^\top (\mathbf{I} - \tilde{\mathbf{A}}) \mathbf{H})\}}{\partial \mathbf{H}} = 0$$

$$\implies (1 - \alpha) \cdot (\mathbf{H} - \mathbf{H}^\circ) + \alpha (\mathbf{I} - \tilde{\mathbf{A}}) \mathbf{H} = 0$$

$$\implies \mathbf{H} = (1 - \alpha) \cdot (\mathbf{I} - \alpha \tilde{\mathbf{A}})^{-1} \mathbf{H}^\circ. \quad (27)$$

By the property of the Neumann series, we have $(\mathbf{I} - \alpha \tilde{\mathbf{A}})^{-1} = \sum_{\ell=0}^{\infty} \alpha^\ell \tilde{\mathbf{A}}^\ell$. Plugging it into Eq. (27) completes the proof. \square

B. *Additional Experiments*

1) *Parameter Analysis:* In this set of experiments, we empirically investigate the impact of three key parameters in LACA (C) and LACA (E): the restart factor α , parameter σ , and the dimension k of TNAM vectors. For each of them, we run LACA (C) and LACA (E) over *Cora*, *PubMed*, *BlogCalaog*, *Flickr*, and *ArXiv*, respectively, by varying the parameter with others fixed.

Varying α . Figs. 9(a) and 9(b) show the precision achieved by LACA (C) and LACA (E) on five datasets, respectively, when α is varied from 0.0 to 0.9 with step size 0.1. It can be clearly observed that both LACA (C) and LACA (E) present nearly identical behaviors on all datasets when varying α . That is, the precision scores increase conspicuously with α increasing. The only exception is on *BlogCL*, where the best result is attained when $\alpha = 0.8$. Recall that in Algo. 2, when α is small, AdaptiveDiffuse will convert substantial residuals into reserves of nearby nodes and distribute only a few to far-reaching neighbors, yielding local clusters with diminutive size, and hence, sub-par result quality.

Varying σ . Next, we study the parameter σ for balancing greedy and non-greedy operations in AdaptiveDiffuse. Recall that a large σ indicates running more greedy operations in AdaptiveDiffuse, which degrades to GreedyDiffuse when $\sigma = 1$. Figs. 9(c) and 9(d) plot the precision scores when increasing σ from 0.0 to 1.0 in LACA (C) and LACA (E), respectively, on five datasets. We can observe that both LACA (C) and LACA (E) (i) are not

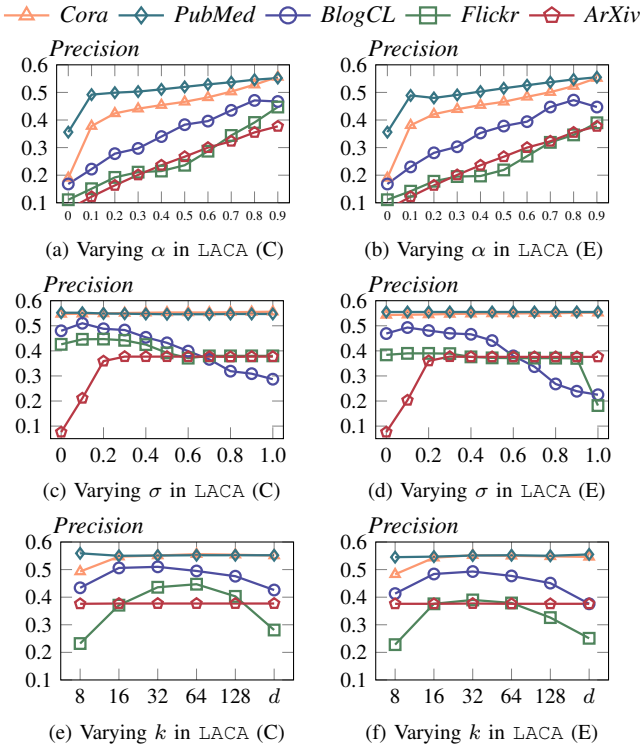


Fig. 9: Precision when varying parameters.

sensitive to σ on *Cora* and *PubMed*, (ii) undergo a significant performance downturn when σ is beyond 0.1 on *BlogCatlog* and *Flickr*, and (iii) on *ArXiv*, see a considerable uptick in precision when σ rises from 0 to 0.2 and invariant results afterward. LACA (C) and LACA (E) favor a small σ on *BlogCatlog* and *Flickr* datasets with high average degrees ($m/n > 60$) because greedy operations are sensitive to high-degree nodes and tend to return small local clusters on such graphs (i.e., fewer non-zero entries in \vec{q}), as analyzed in Section IV-A.

Varying k . Figs. 9(e) and 9(f) show the precision values of LACA (C) and LACA (E) when varying the dimension k of TNAM vectors \mathbf{Z} in $\{8, 16, 32, 64, 128, d\}$. On citation networks *Cora*, *PubMed*, and *ArXiv*, we can see that the performance of both LACA (C) and LACA (E) remains stable when k is increased from 8 to d , except a slight drop on *Cora* when $k = 8$. In comparison, on social networks *BlogCL* and *Flickr*, a remarkable improvement and reduction in performance can be observed when k increases from 8 to 32 and from 32 to d , respectively. The reason is that both *BlogCL* and *Flickr* have numerous distinct attributes in \mathbf{X} ($d = 8, 189$ and $d = 12, 047$), which embody substantial noisy information. Meanwhile, our k -SVD essentially denoises attribute data by extracting k key components. The observations manifest the effectiveness of our TNAM construction technique (Section V-A) in capturing the attribute similarity of node pairs with a small dimension k , e.g., 16 or 32.

2) **Ablation Study:** To study the effectiveness of the SNAS in our BDD definition (Eq. (5)), our graph diffusion algorithm AdaptiveDiffuse in Section IV-C, as well as the k -

SVD in Section V-A, we create three ablated versions for LACA (C) and LACA (E), respectively. Particularly, the variants of LACA (C) and LACA (E) without AdaptiveDiffuse are implemented using GreedyDiffuse as the diffusion component.

Table VI reports the best precision scores attained by each method on 8 datasets. We can see remarkable performance decreases in both LACA (C) and LACA (E) after disabling any of these three ingredients, especially the SNAS. The only exception is on *Amazon2M*, where LACA (C) achieves a better result when SNAS is removed from BDD, whereas LACA (E) exhibits a radically different phenomenon. This indicates that the exponential cosine similarity is more robust in modelling the similarity of node attributes. From Table VI, AdaptiveDiffuse is another key component affecting the resulting quality, which accords with our analysis of GreedyDiffuse’s deficiencies in Section IV-C. Consistent with the observations from Figs. 9(e) and 9(f), the k -SVD in Algo. 3 improves the performance of LACA due to its denoising ability.

TABLE VI: Ablation study. Darker shades indicate better results.

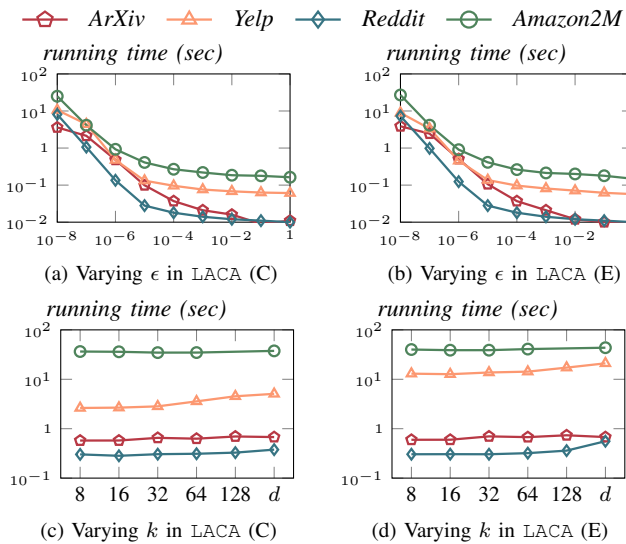
Method	<i>Cora</i>	<i>PubMed</i>	<i>BlogCL</i>	<i>Flickr</i>	<i>ArXiv</i>	<i>Yelp</i>	<i>Reddit</i>	<i>Amazon2M</i>
LACA (C)	0.556	0.552	0.51	0.447	0.377	0.754	0.808	0.465
w/o k -SVD	0.551	0.552	0.426	0.281	0.377	0.754	0.808	0.465
w/o AdaptiveDiffuse	0.544	0.551	0.48	0.426	0.329	0.754	0.213	0.287
w/o SNAS	0.486	0.537	0.302	0.2	0.343	0.687	0.779	0.495
LACA (E)	0.552	0.555	0.493	0.39	0.377	0.739	0.808	0.521
w/o k -SVD	0.546	0.554	0.395	0.251	0.376	0.737	0.808	0.514
w/o AdaptiveDiffuse	0.54	0.553	0.469	0.384	0.336	0.735	0.214	0.365
w/o SNAS	0.486	0.537	0.302	0.2	0.343	0.687	0.779	0.495

3) **Conductance and WCSS:** This set of experiments studies the average *conductance* [23] and the average *within-cluster sum of squares* (WCSS) [87] of ground-truth and the local clusters output by LACA (C), LACA (E), and 17 competitors. Given a local cluster C_s , conductance only measures the connectivity between nodes in C_s and nodes outside C_s , while WCSS merely evaluates the variance of attribute vectors of nodes in C_s . Intuitively, lower conductance and WCSS indicate a higher clustering quality. The conductance and WCSS values of all methods on the eight datasets are reported in Table VII. We highlight the top 3 best results (with the smallest differences from the ground truth) on each dataset in blue, with darker shades indicating higher quality. From Table VII, we can see that none of the evaluated methods perform best on all datasets. But notably, LACA (C) and LACA (E) obtain the top 3 conductance or WCSS results on eight and seven datasets, respectively, whereas the best competitor PR-Nibble is ranked in the top 3 on six datasets, meaning that local clusters by LACA achieve a good balance of structure cohesiveness and attribute homogeneity. Another observation is that compared to WCSS, conductance values by different methods vary markedly. This is because nodes in a graph have divergent degrees, and hence, a small change in a cluster can lead to a large difference in conductance.

4) **Scalability Evaluation:** This section experimentally evaluates the scalability of LACA (C) and LACA (E) on four

TABLE VII: Conductance and WCSS.

Method	Cora		PubMed		BlogCL		Flickr		ArXiv		Yelp		Reddit		Amazon2M	
	Cond. ↓	WCSS ↓	Cond. ↓	WCSS ↓	Cond. ↓	WCSS ↓	Cond. ↓	WCSS ↓	Cond. ↓	WCSS ↓	Cond. ↓	WCSS ↓	Cond. ↓	WCSS ↓	Cond. ↓	WCSS ↓
Ground-truth	0.188	0.979	0.204	0.976	0.608	0.963	0.765	0.997	0.408	0.663	0.649	0.55	0.226	0.594	0.173	0.981
PR-Nibble [15]	0.337	0.966	0.199	0.974	0.569	0.969	0.733	0.998	0.518	0.667	0.237	0.55	0.368	0.595	0.369	0.984
APR-Nibble	0.323	0.964	0.196	0.974	0.671	0.964	0.799	0.99	0.345	0.475	0.345	0.475	0.583	0.428	0.409	0.937
HK-Relax [16]	0.138	0.966	0.096	0.971	0.481	0.967	0.748	0.998	0.222	0.663	0.13	0.556	0.196	0.583	0.132	0.946
CRD [20]	0.156	0.942	0.173	0.947	0.61	0.967	0.787	0.974	0.28	0.644	0.139	0.563	0.275	0.588	0.168	0.928
p -Norm FD [21]	0.131	0.954	0.178	0.958	0.709	0.967	0.845	0.996	0.252	0.656	0.35	0.404	0.235	0.593	0.118	0.971
WFD [33]	0.127	0.956	0.17	0.96	0.713	0.964	0.845	0.996	0.251	0.657	0.339	0.405	0.468	0.508	0.145	0.971
Jaccard [54]	0.617	0.984	0.637	0.981	0.655	0.969	0.854	0.998	0.846	0.682	0.696	0.58	0.744	0.66	0.707	0.993
Adamic-Adar [54]	0.617	0.984	0.637	0.981	0.609	0.969	0.584	0.998	0.834	0.682	0.696	0.58	0.771	0.654	0.707	0.993
Common-Nbrs [54]	0.617	0.984	0.637	0.981	0.594	0.969	0.573	0.998	0.834	0.682	0.696	0.58	0.777	0.654	0.707	0.993
SimRank [55]	0.265	0.98	0.226	0.978	0.723	0.968	0.954	0.998	-	-	-	-	-	-	-	-
SimAttr (C) [56]	0.714	0.975	0.469	0.974	0.816	0.965	0.729	0.998	0.811	0.683	0.673	0.522	0.704	0.573	0.702	0.986
SimAttr (E) [57]	0.714	0.975	0.469	0.974	0.816	0.965	0.729	0.998	0.811	0.683	0.673	0.522	0.704	0.573	0.702	0.986
AttriRank [58]	0.816	0.985	0.654	0.98	0.818	0.968	0.891	0.998	0.925	0.684	0.683	0.576	0.951	0.669	0.86	0.995
Node2Vec [59]	0.194	0.984	0.182	0.979	0.589	0.968	0.739	0.998	0.36	0.67	0.407	0.579	-	-	-	-
GraphSAGE [38]	0.262	0.982	0.338	0.98	0.531	0.969	0.757	0.999	-	-	-	-	0.736	0.573	0.748	0.986
PANE [61]	0.465	0.98	0.376	0.976	0.548	0.967	0.715	0.998	0.841	0.673	0.592	0.562	-	-	-	-
CFANE [62]	0.369	0.979	0.264	0.975	0.754	0.964	0.876	0.998	-	-	-	-	-	-	-	-
LACA (C)	0.227	0.977	0.106	0.975	0.669	0.962	0.824	0.998	0.248	0.664	0.642	0.518	0.254	0.597	0.244	0.985
LACA (E)	0.228	0.977	0.108	0.975	0.661	0.962	0.849	0.992	0.247	0.665	0.494	0.534	0.254	0.598	0.155	0.981

Fig. 10: Efficiency when varying ϵ and k .

large graphs *ArXiv*, *Yelp*, *Reddit*, and *Amazon2M* by varying diffusion threshold ϵ and dimension k .

Fig. 10(a) and 10(b) depict the running times of LACA (C) and LACA (E) on the four datasets when decreasing ϵ from 1 to 10^{-8} , respectively. Specifically, the average runtime of both LACA (C) and LACA (E) increases by roughly an order of magnitude when there is a tenfold decrease in ϵ , which is consistent with our complexity analysis of LACA in Section V-B.

Although LACA (C) and LACA (E) are local algorithms, i.e., their time complexities are independent of n and m , we can observe that under the same ϵ settings, their empirical times vary on datasets with varied sizes. Note that this difference is caused by their diverse graph structures that lead to different data locality and memory access patterns. For example, although *Reddit* contains more nodes and $99\times$ more edges than *ArXiv*, their running times are comparable when $\epsilon \geq 10^{-3}$ and the cost for *ArXiv* turns to be markedly higher than that for *Reddit* when $10^{-7} \leq \epsilon \leq 10^{-4}$. The reason is that nodes in *ArXiv* are sparsely connected, making the

matrix-vector multiplications in Algo. 2 inefficient. As for *Yelp* and *Amazon2M*, they encompass significantly more nodes and edges than *ArXiv* and *Reddit*, and, hence, are more likely to yield cache misses and intensive memory access patterns that result in lower efficiency.

In Fig. 10(c) and 10(d), we display the running times of LACA (C) and LACA (E) when increasing k from 8 to d . Notably, the time required by LACA (C) and LACA (E) remains stable when varying k in $\{8, 16, 32, 64, 128\}$, indicating that the time cost of LACA is dominated by $1/\epsilon$ when k is not large.

TABLE VIII: Statistics of Datasets without Attributes.

Dataset	n	m	$ \mathcal{Y}_s $
<i>com-DBLP</i> [88]	317,080	1,049,866	1,862
<i>com-Amazon</i> [88]	334,863	925,872	47
<i>com-Orkut</i> [88]	3,072,441	117,185,083	621

TABLE IX: The average precision evaluated with ground-truth. Best is **bolded** and best baseline underlined.

Method	<i>com-DBLP</i> [88]	<i>com-Amazon</i> [88]	<i>com-Orkut</i> [88]
PR-Nibble [15]	0.374	0.835	0.251
HK-Relax [16]	0.305	0.865	0.233
CRD [20]	0.247	0.696	0.021
p -Norm FD [21]	0.331	0.871	0.199
LACA (w/o SNAS)	0.399	0.919	0.253

5) Quality Evaluation on Graphs without Attributes:

This set of experiments evaluates the performance of LACA (i.e., LACA (w/o SNAS)) against 4 strong LGC baselines (PR-Nibble, HK-Relax, CRD, and p -Norm FD) on graphs without node attributes in terms of local clustering quality, using the same evaluation protocol in Section VI-B. Table VIII lists the statistics of the non-attributed graph datasets of various volumes and types for evaluation [88]. In *com-DBLP*, the nodes represent authors, and the edges represent co-authorship between published authors. The ground-truth clusters are formed based on the publication venue. *com-Amazon* is a co-purchasing network where products are nodes, and edges represent frequently co-purchased items.

The ground-truth clusters are determined by product categories. *com-Orkut* is a social network where users establish friendships and join groups. The groups created by users are considered the ground-truth clusters.

The average precisions of the local clusters produced by LACA and 4 competitors are presented in Table IX. It can be observed that LACA consistently delivers the best performance across all three datasets. Specifically, on the medium-sized datasets *com-DBLP* and *com-Amazon*, LACA surpasses the best competitors, PR-Nibble and p -Norm FD, by a significant gain of 2.5% and 4.8% in precision, respectively. On the large graph *com-Orkut* with 117.2 million edges, LACA still outperforms the state-of-the-art baseline PR-Nibble with an improvement of 0.2%. The results manifest that our proposed BDD in LACA can accurately capture the affinity between nodes even without node attributes through the bidirectional random walks that consider the node importance from the perspectives of both, as remarked in Section II-C.

C. Alternative Implementation of LACA

TABLE X: The average precision comparing with alternative BDD implementations.

Method	Cora	PubMed	BlogCL	Flickr	ArXiv	Yelp	Reddit	Amazon2m
LACA (C)	0.556	0.552	0.51	0.447	0.377	0.754	0.808	0.465
LACA (C)-RS-RS-RS	0.181	0.383	0.167	0.121	0.091	0.737	0.054	0.227
LACA (C)-R-RS-RS	0.224	0.446	0.184	0.152	0.209	0.737	0.194	0.223
LACA (C)-RS-R-RS	0.222	0.441	0.18	0.142	0.169	0.737	0.114	0.225
LACA (C)-RS-RS-R	0.194	0.360	0.174	0.145	0.082	0.720	0.065	0.237
LACA (E)	0.552	0.555	0.493	0.39	0.377	0.739	0.808	0.521
LACA (E)-RS-RS-RS	0.17	0.358	0.167	0.11	0.091	0.737	0.058	0.133
LACA (E)-R-RS-RS	0.179	0.364	0.178	0.113	0.208	0.737	0.191	0.396
LACA (E)-RS-R-RS	0.181	0.365	0.177	0.11	0.167	0.719	0.11	0.243
LACA (E)-RS-RS-R	0.183	0.352	0.172	0.113	0.082	0.719	0.064	0.133

TABLE XI: Ablation study on various similarity measures.

Method	Cora	PubMed	BlogCL	Flickr	ArXiv	Yelp	Reddit	Amazon2m
LACA (C)	0.556	0.552	0.51	0.447	0.377	0.754	0.808	0.465
LACA (E)	0.552	0.555	0.493	0.39	0.377	0.739	0.808	0.521
LACA (Jaccard)	0.524	✗	0.304	0.28	✗	✗	✗	✗
LACA (Pearson)	0.518	0.551	0.289	0.115	-	-	-	-

1) *Alternative Implementation of BDD*: To rigorously validate the effectiveness of our BDD, we have implemented the new graph diffusion algorithms for local clustering based on the suggested formulation in the comment and the other three alternative formulations as follows:

- 1) RS-RS-RS: Integrating attribute similarity (i.e., SNAS) into all three random walk steps as suggested. Specifically, for each node pair (v_s, v_t) , the affinity is defined by $\sum_{v_i, v_j \in V} \rho(v_s, v_i) \cdot \rho(v_i, v_j) \cdot \rho(v_t, v_j)$, where $\rho(v_i, v_j) = \begin{cases} \pi(v_i, v_j) \cdot s(v_i, v_j) & \text{if } v_i \text{ is connected to } v_j \text{ via an edge} \\ 1 & v_i = v_j \end{cases}$.
- 2) R-RS-RS: Integrating attribute similarity (i.e., SNAS) into the second and third random walk steps. For each node pair (v_s, v_t) , the affinity is defined by $\sum_{v_i, v_j \in V} \pi(v_s, v_i) \cdot \rho(v_i, v_j) \cdot \rho(v_t, v_j)$.
- 3) RS-R-RS: Integrating attribute similarity (i.e., SNAS) into the first and third random walk steps. For each node pair (v_s, v_t) , the affinity is defined by $\sum_{v_i, v_j \in V} \rho(v_s, v_i) \cdot \pi(v_i, v_j) \cdot \rho(v_t, v_j)$.

- 4) RS-RS-R: Integrating attribute similarity (i.e., SNAS) into the first and second random walk steps. For each node pair (v_s, v_t) , the affinity is defined by $\sum_{v_i, v_j \in V} \rho(v_s, v_i) \cdot \rho(v_i, v_j) \cdot \pi(v_t, v_j)$.

and have compared them against our original BDD.

Table X reports the local clustering performance of LACA (C) and LACA (E) based on our BDD and the above four alternative definitions. It can be observed that all these four variants undergo severe performance degradation compared to the BDD on most datasets. For instance, on *Cora* and *Amazon*, LACA (C)-BDD is able to yield 55.6% and 46.5% in precision, whereas the four alternatives achieve at most 22.4% and 23.7%, respectively. The remarkable superiority of the BDD over the alternatives is due to the fact that these alternatives overly incorporate the attribute similarity (at least two attribute-only transitions) and topological connectivity (three random walk steps) into the random walk diffusion process, rendering the graph traversal rather biased and easier to jump to the nodes that are distant or even disconnected from the seed node v_s via the intermediate nodes with high attribute similarities and long random walks. In turn, it is more likely to produce nodes that are far-reaching from the local cluster around v_s .

2) *Alternative Choices on Similarity Measurements*: To further demonstrate the superiority of LACA (C) and LACA (E), we have conducted an ablation study that employs the Jaccard and Pearson correlation coefficients as the SNAS in LACA (C) and LACA (E) on all datasets. Note that the Jaccard coefficient requires the attribute values to be binary and thus are not applicable to datasets with continuous attributes, i.e., *PubMed*, *ArXiv*, *Yelp*, *Reddit*, and *Amazon2M* and the Pearson correlation coefficient is unable to report the results on large graphs within three days due to the high complexity ($O(n^2d)$) needed for calculating the similarities of the intermediate node pairs. As presented in Table XI, LACA (C) and LACA (E) consistently outperform these two variants with considerable gains. For example, on *Flickr*, LACA (C) can obtain a precision of 44.7%, while the precision scores attained by Jaccard and Pearson correlation coefficients are merely 28% and 11.5%.

D. Other Related Work

1) *Attributed Network Embedding*: Attributed network embedding (ANE) is to embed each node graph \mathcal{G} into a low-dimensional feature vector, preserving both topology and attribute information. The obtained embeddings can be used in many downstream tasks, including graph clustering. ANE methods can be categorized into two types: factorization-based and learning-based. Factorization-based methods [61], [89]–[91] construct and factorize node proximity matrices that integrate graph topology and node attributes to derive low-dimensional vectors. TADW [89] leverages a second-order adjacency matrix, AANE [90] matches node representations with attribute proximities, PANE [60], [61] optimizes forward and backward affinity matrices via random walks and optimizes convergence with greedy initial technique. However, these methods suffer from scalability issues due to the necessity

of factorization of an $n \times n$ proximity matrix. Learning-based methods [38], [62], [92], [93] are further classified into encoder-decoder and propagation categories. Encoder-decoder methods, including DANE [93] and ANRL [92], integrate attribute features and graph topology by utilizing multiple autoencoders to minimize input reconstruction loss. Additionally,

ANRL develops an attribute-aware model based on the Skip-gram model [94]. CFANE [62] integrates propagation-based and encoder-decoder methods, utilizing self-attention to refine its model. In contrast to our local-based approach, these ANE methods typically require processing nodes across the entire graph.